Genetic incompatibilities and reduced transmission in chickens may limit the evolution of reassortants between H9N2 and panzootic H5N8 clade 2.3.4.4 avian influenza virus showing high virulence for mammals

Ahmed Mostafa,[1,2,*,†] Claudia Blaurock,[3,†] David Scheibner,[3] Christin Müller,[1] Ulrike Blohm,[4] Alexander Schäfer,[4] Marcel Gischke,[3] Ahmed H. Salaheldin,[3] Hanaa Z. Nooh,[5] Mohamed A. Ali,[2] Angele Breithaupt,[6] Thomas C. Mettenleiter,[3] Stephan Pleschka,[1] and Elsayed M. Abdelwhab[3,*,‡]

[1]Institute of Medical Virology, Justus Liebig University Giessen, Schubertstrasse 81, 35392 Giessen, Germany, [2]Center of Scientific Excellence for Influenza Viruses, National Research Centre (NRC), Dokki, 12622, Giza, Egypt, [3]Institute of Molecular Virology and Cell Biology and , [4]Institute of Immunology, Friedrich-Loeffler-Institut, Federal Research Institute for Animal Health, Südufer 10, 17493 Greifswald-Insel Riems, Germany, [5]Department of Anatomy and Histology, College of Medicine, Jouf University, Sakaka 72442, Aljouf Province, Saudi Arabia and [6]Department of Experimental Animal Facilities and Biorisk Management, Friedrich-Loeffler-Institut, Federal Research Institute for Animal Health, Südufer 10, 17493 Greifswald-Insel Riems, Germany

*Corresponding author: E-mail: sayed.abdel-whab@fli.de or ahmed_elsayed@daad-alumni.de

†Ahmed Mostafa and Claudia Blaurock contributed equally to this work. Author order was determined both alphabetically and in order of seniority.

‡https://orcid.org/0000-0003-2103-0922

Abstract

The unprecedented spread of H5N8- and H9N2-subtype avian influenza virus (AIV) in birds across Asia, Europe, Africa, and North America poses a serious public health threat with a permanent risk of reassortment and the possible emergence of novel virus variants with high virulence in mammals. To gain information on this risk, we studied the potential for reassortment between two contemporary H9N2 and H5N8 viruses. While the replacement of the PB2, PA, and NS genes of highly pathogenic H5N8 by homologous segments from H9N2 produced infectious H5N8 progeny, PB1 and NP of H9N2 were not able to replace the respective segments from H5N8 due to residues outside the packaging region. Furthermore, exchange of the PB2, PA, and NS segments of H5N8 by those of H9N2 increased replication, polymerase activity and interferon antagonism of the H5N8 reassortants in human cells. Notably, H5N8 reassortants carrying the H9N2-subtype PB2 segment and to lesser extent the PA or NS segments showed remarkably increased virulence in mice as indicated by rapid onset of mortality, reduced mean time to death and increased body weight loss. Simultaneously, we observed that in chickens the H5N8 reassortants, particularly with the H9N2 NS segment, demonstrated significantly reduced transmission to co-housed chickens. Together, while the limited capacity for reassortment between co-circulating H9N2 and H5N8 viruses and the reduced bird-to-bird transmission of possible H5N8 reassortants in chickens may limit the evolution of such reassortant viruses, they show a higher replication potential in human cells and increased virulence in mammals.

Importance

The segmented nature of avian influenza viruses (AIV) genome enables the evolution of new virus variants by exchanging segments (reassortment) between two viruses upon co-infection of the same host-cell. Reassortment resulted in the evolution of pandemic and highly virulent influenza viruses in humans. Here, we studied the potential reassortment of two German AIV H5N8 and H9N2 and the impact on virus fitness in human cells, mice, and chickens. We found that H9N2 PB1 and NP were not compatible to replace the respective segments from H5N8, interestingly, due to genetic differences outside the packaging region. Importantly, H5N8 viruses carrying H9N2 PB2, PA, and NS segments exhibited high adaptation in human cells and remarkably increased virulence in mice. However, the reassortment between H5N8 and H9N2 negatively affected transmission in chickens. This study is important for zoonotic risk assessment after reassortment of H5N8 and H9N2 AIV similar to those used in this study.

1. Introduction

Avian influenza viruses (AIV) are members of the genus influenza A virus (IAV) in the family *Orthomyxoviridae*. The single-stranded negative-sense RNA genome consists of eight segments, which encode at least 10 viral proteins (Bouvier and Palese 2008) divided into two categories: structural (i.e. part of the virion) and non-structural components. The virion consists of the internal ribonucleoprotein (RNP) complex (encompassing polymerase basic subunit 1 (PB1) and subunit 2 (PB2), polymerase acidic protein (PA), nucleoprotein (NP), and viral RNA), the matrix protein 1 (M1), and the nuclear export protein (NEP). The virion envelope contains the hemagglutinin (HA), neuraminidase (NA), and matrix protein 2 (M2). Several non-structural proteins (e.g. NS1, PB1-F2, and PA-x) are not packaged into the virus particles, but are expressed in the host cell, and play important roles, for example, in interferon-antagonism, inflammatory response, or apoptosis. Some non-structural proteins are not necessarily present upon infection with every influenza virus (e.g. PB1-F2) (Bouvier and Palese 2008). The HA and NA of IAV are classified into 18 and 11 distinct subtypes, respectively (Bouvier and Palese 2008). H17, H18, N10, and N11 have not been found in avian species. The majority were identified in AIV from wild birds but also frequently isolated in poultry. While most of AIV exhibit low pathogenicity (LP) in the wild bird reservoir, AIV specifying H5 and H7 can become highly pathogenic (HP) after circulation of LP precursors in poultry (Alexander 2000). Due to the segmented nature of the viral genome, these segments can be exchanged (i.e. reassortment) between different viruses upon co-infection of the same host leading to the evolution of new virus variants with altered characteristics. Reassortment has resulted in strains that have caused pandemic outbreaks with devastating impacts on the human population (Mostafa et al. 2018).

H9N2 is the most widespread AIV subtype in poultry worldwide. Several clades of AIV H9N2 (e.g. G1, Y280, Korean or European lineages) are endemic in many countries in Asia, Europe and the Middle East (Fusaro et al. 2011). In poultry, some Asian H9N2 viruses exhibited mild-to-moderate virulence with or without co-infections with other viruses or bacteria (Guo et al. 2000; Kishida et al. 2004; Lee et al. 2011). Moreover, H9N2 viruses were isolated from humans in several countries (Freidl et al. 2014; Nagy, Mettenleiter, and Abdelwhab 2017). Importantly, H9N2 viruses donated internal segments to other AIV generating zoonotic reassortant viruses, like AIV A/Goose/Guangdong/1/1996 H5N1 (GsGD96) (Guan et al. 1999), the 2013 H10N8 (Chen et al. 2014), and the continuously circulating 2013 H7N9 (Pu et al. 2015).

GsGD96-like viruses continue to pose a serious public health threat. From 1996 to date, the virus evolved into 10 phylogenetic clades (clade 0 to 9) and multiple subclades. While most of these subclades disappeared, clade 2.3.4.4 viruses are still circulating in wild and domestic birds. Since 2009, the reassortment of the H5 HA segment of clade 2.3.4.4 with other AIV subtypes resulted in the evolution of H5N1-, H5N2-, H5N3-, H5N5-, H5N6- and H5N8-subtypes in wild and domestic birds (Lee et al. 2017). These viruses have spread from South Korea and China to many Asian, European, and North American countries. This panzootic spread of AIV H5 clade 2.3.4.4 was alarming for both poultry and human health. Although the pathogenicity of clade 2.3.4.4 H5Nx viruses in mammals varied considerably, some viruses (e.g. H5N6, H5N2) were able to infect mammals including humans causing mild to fatal infections (Kim et al. 2014; Pulit-Penaloza et al. 2015; Kaplan et al. 2016; Pan et al. 2016; Wang et al. 2016, 2017; Kwon et al. 2018; Lee et al. 2018). Interestingly, unlike human-pathogenic H7N9 or H10N8 AIVs (Guan et al. 1999; Chen et al. 2014; Pu et al. 2015), sequence analysis of the H5N8 clade 2.3.4.4 indicated no relationship to H9N2-derived segments (Kwon et al. 2018). Since 2016, an unprecedented number of H5N8 clade 2.3.4.4 outbreaks was reported in birds in Europe (Napp et al. 2018; Pohlmann et al. 2018), where H9N2 is semi-endemic posing a continuous risk for reassortment (Reid et al. 2016; Świętoń et al. 2018). The reassortment of avian and human transmission influenza viruses may result in the occurrence of influenza pandemics, since the human population is naïve for such viruses and high mortality rates are expected (Mostafa et al. 2018). The relevance of a scenario is highlighted by the fact that pandemic influenza viruses in 1957, 1968, and 2009 possessed segments, particularly PB2, PB1, and/or PA, from avian origin viruses (Mostafa et al. 2018).

Here, we studied the impact of potential reassortment between two recent German H5N8 clade 2.3.4.4 and H9N2 viruses on replication in human cells and virulence in mice and chickens.

2. Materials and methods

2.1 Viruses and cells

German H5N8, H9N2, and Tk14 were provided by Timm Harder at FLI, Riems and H9N2-G1-like was obtained from the Center of Scientific Excellence for Influenza Viruses, National Research Centre, Egypt. MDCK-II and HEK293T were obtained from the cell culture collection at FLI Insel Riems. Calu-3 and A549 were obtained from the Institute of Medical Virology, Justus Liebig

University Giessen, Germany. NHBE (Lonza) were prepared according to manufacturer's instructions. CEK cells were prepared from 18-day-old SPF embryonated chicken eggs (VALO BioMedia) (Hennion and Hill 2015).

2.2 Generation of Recombinant Viruses

All genomic segments of H5N8 and H9N2 were amplified and cloned in pHW vector and viruses were rescued in MDCK-II and HEK293T cells (Stech et al. 2008; Mostafa et al. 2015). H9N2 was rescued and propagated in cell culture in the presence of N-tosyl-L-phenylalanine chloromethyl ketone (TPCK)-trypsin. All viruses were propagated in 9- to 11-day-old SPF eggs and viruses were maintained at −80°C until use.

2.3 Sequence Analysis

RNA of recombinant viruses was extracted using the QIAamp Viral RNA Mini Kit and transcribed into cDNA using the Omniscript Reverse Transcription Kit (Qiagen). All segments were purified from gel slices after Phusion RT-PCR (Stech et al. 2008) using the Qiagen Gel Extraction Kit (Qiagen) and subjected for Sanger sequencing using the ABI BigDye Terminator v.1.1 Cycle Sequencing Kit (Applied Biosystems). Sequences of German viruses in this study were submitted to GISAID and assigned isolate identity numbers 486439, 486440, and 486441. The Egyptian H9N2 virus had NCBI accession numbers MK190705 to MK190710 for the internal gene segments. Comparison between H9N2 and H5N8 genomes was done by Geneious v.11.1.5 (Biomatters). Tertiary structures of PB1 and NP were generated using SWISS-Model (https://swissmodel.expasy.org) and PyMol software (https://pymol.org).

2.4 Replication kinetics in primary human and chicken cells

NHBE cells were differentiated under air-liquid conditions as described (Matrosovich et al. 2004). NHBE and CEK were infected with recombinant viruses at an MOI of 0.01 for the indicated time periods. TPCK-trypsin was added for the replication of H9N2 in CEK, but not in NHBE cells. Cells were harvested and the virus titer was determined using foci assay (FA) (Ma et al. 2010). TPCK-trypsin was used for the titration of H9N2 only. The test was performed in triplicates and in three independent biological replicates. Each sample was titrated in duplicates.

2.5 Replication kinetics in human cells

Replication of recombinant H5N8/H9N2 viruses in human cells was determined in A549 and Calu-3 cells infected at an MOI of 0.01 for 1h. The inoculum was removed and cells were treated with citrate buffer saline pH 3 and washed using phosphate buffer saline (PBS, MP Biomedicals). Minimal essential medium (MEM) containing 0.2 per cent bovine serum albumin (BSA) was added and cells were incubated for the indicated time periods at 33°C, 37°C, and/or 39°C. TPCK-trypsin was added for the replication of H9N2 in A549 cells. Cell culture supernatants were harvested and stored at −80°C until titration.

2.6 Virus titration

Virus titration in this study was determined by plaque assay in MDCK-II cells (Abdelwhab et al. 2016) except for replication in human cell culture which was performed by FA as described

(Ma et al. 2010). TPCK-trypsin was added for the titration of H9N2 only.

2.7 Minigenome luciferase assay

The luciferase assay was performed using Dual-Luciferase Reporter Assay System (Promega) (Petersen et al. 2018). Briefly, confluent HEK293T cells were transfected with 1 µg of PB2, PB1, PA, and NP from H5N8 and/or H9N2 or empty pHW2000 plasmids mixed with 40 ng Renilla luciferase expression plasmid pRL-SV40 (Promega) and 200 ng p125-Luc Firefly luciferase expression plasmid containing the luciferase reporter gene (Yoneyama et al. 1998). Transfection was performed using Trans-IT2020 (Mirus) for 8h at 33°C and 39°C (Mostafa et al. 2013). Relative luminometer units (RLU) of each reaction were normalized to Renilla luciferase and the results are expressed as x-fold change compared to the negative control.

2.8 Detection of interferon-beta (IFN-β) response in cell culture

Amplification of the IFN-β mRNA in A549 infected with the indicated viruses at an MOI of 1 for 24h was done as previously published (Petersen et al. 2018). The relative expression in infected and non-infected cells was calculated using the $2^{\wedge}\text{-}(\Delta\Delta ct)$ method (Livak and Schmittgen 2001).

2.9 Flow cytometry

A549 cells were infected at an MOI of 1 with H5N8, H5N8_NS, and H5N8_PB2-PA-NS at 33°C or 39°C. At 24 hpi, cells and supernatant were harvested and centrifuged at 1,100 rpm for 5 min and washed with PBS. Separated cells were stained with live/dead dye Zombie Aqua™ Fixable (Biolegend) for 20 min, then washed with MEM media containing 10 per cent FCS and fixed and permeabilized with True-Nuclear™–reagent (Biolegend) for 30 min. Cells were stained with primary mouse-anti-NP antibody (ATCC-HB65) for 30 min followed by rat-anti-mouse IgG2a-PE (Dianova) as secondary antibody for 30 min. Cells were washed with FACS-Buffer and analyzed via FACS. Cells were analyzed by excluding doublets (FSC-A vs. FSC-H) and dead cells (Zombie Aqua+).

2.10 Ethic statement

Experiments were carried out in the biosafety level-3 animal facilities of the FLI according to the German Regulations for Animal Welfare and after approval of the authorities (permission number: 7221.3-1-060/17) and the commissioner for animal welfare at the FLI representing the Institutional Animal Care and Use Committee (IACUC).

2.11 Infection of mice

Four-week-old female BALB/C mice (Charles River) were allocated in closed ISOcage system (Tecniplast) and were left to adapt for 5 days before challenge. At the day of challenge (d0), all mice were weighed and individually marked. For each virus, mice received either 10^5 ($n = 11$) or 10^3 ($n = 8$) pfu in 50 µl MEM. One control group ($n = 8$) received 50 µl sterile medium (sham group). Inoculation was performed under mild anesthesia using Isoflurane (CP-Pharma). Mice were observed daily for clinical signs and the daily BW per gram was expressed relative to the BW of each mouse at d0. All mice that had lost more than 25 per cent of the d0-BW were humanely killed and scored dead. After

3 dpi, three mice per group were euthanized using isoflurane. The whole brain, one lung, and half of the spleen were collected and homogenized using TissueLyzer® (Qiagen) at ratio 1 g/1 ml PBS and stored at −80 °C until further use. The second half of the spleen was used for flow cytometry analysis. The experiment ran for 11 dpi, all surviving mice were humanely killed using isoflurane and cervical dislocation. MTD was calculated.

2.12 Virus replication in mice

Brain, lungs, and spleen of mice were weighed (w/v) and homogenized and the virus titer was determined by plaque assay. Viral RNA was extracted automatically by RNA Extraction Kit (Macherey Nagel). The amount of viral RNA in homogenized samples was also detected by RT-qPCR (Hoffmann et al. 2016).

2.13 Detection of IFN-β response in the lung of mice

Lungs were collected at 3 dpi, weighed (w/v), and homogenized. The total RNA was extracted from homogenized lung tissues using Trizol and RNeasy Kit (Qiagen). The cDNA was synthesized from 400 ng RNA using the Prime Script 1st Strand cDNA Synthesis Kit (TaKaRA) and Oligo dT Primer (TaKaRa). Quantification of IFN-β transcripts was done using SYBR® GreenER™ qPCR SuperMIX Universal Kit (Invitrogen) and generic primers (Kim et al. 2003; Li, Moltedo, and Moran 2012). The x-fold change of normalized samples to β-actin transcripts (Petersen et al. 2018) compared to the control mice was calculated using the 2^-(ΔΔct) method.

2.14 Detection of cell-mediated immunity in the spleen of mice

At 3 dpi, the spleen was removed and single cell suspensions were prepared for flow cytometry analysis. T-cell subsets and activation status were identified with fluorescent dye-labeled antibodies against the following murine surface antigens: CD3 (clone 17A2), APC-Cy7; CD4 (clone GK1.5), FITC; CD8 (clone 53-6.7), APC; CD69 (clone H1.2F3), PE-Cy7 (Biolegend). All incubation steps were carried out for 15 min at 4 °C in the dark. The iNKT cell subtype was detected by PE-labeled, empty or PBS57-loaded, CD1d Tetramer (NIH tetramer Core Facility). For iNKT staining, tetramers were incubated for 30 min, in the dark. Cells were washed in fluorescence-activated cell sorting (FACS) buffer and analyzed by Flow cytometer BD Fortessa and FACS DIVA software (BD Biosciences).

2.15 Infection of chickens

Six-week-old SPF chickens were randomly allocated into six groups. Ten chickens were inoculated with $10^{3.7}$ pfu/bird and five naïve birds were added at 1 dpi to each group. Birds were observed daily for morbidity and mortality. Clinical scoring was given and the PI and MTD were calculated as previously done (Abdelwhab el al. 2016). Chickens were kept on the floor in separate rooms (one group per room) at the BSL3 facilities of the FLI. In each room, water was supplied with cup and bell drinkers and feed was provided in wide grid metal troughs and flat containers. Temperature and light were regulated automatically and all stables were cleaned daily by water. Each room contained a video camera.

2.16 Virus excretion and seroconversion

Swabs were collected from surviving or freshly dead birds and virus titer was determined by plaque assay. Furthermore, detection of viral RNA was determined as previously described (Hoffmann et al. 2016) after automatic extraction. Sera collected at the end of experiments were examined using 'ID screen Influenza A Antibody Competition Multispecies Kit' enzyme-linked immunosorbent assay (ELISA) (IDvet) in Infinite® 200 PRO reader (TECAN).

2.17 Histopathology and immunohistochemistry

Tissues from chickens ($n = 3$ per group) inoculated with H5N8, H5N8_NS, or H5N8_PB2-PA-NS were collected in 10 per cent neutral phosphate buffer formalin. Sample processing, hematoxylin and eosin (HE) staining, and immunohistochemistry was performed as published (Breithaupt et al. 2011), but with using a monoclonal antibody against the M protein of IAV (ATCC clone HB-64, 1:200, at 4 °C overnight). Necrosis was scored on a scale 0 to 3+: 0 = no lesion, 1+ = mild, 2+ = moderate, 3+ = severe. Viral antigen was scored on a labeling scale 0 to 3+: 0 = negative, 1+ = focal to oligofocal, 2+ = multifocal, 3+ = coalescing foci or diffuse labelling (blinded study).

2.18 Statistics

Statistical analysis for swab and organ samples, replication kinetics, immune response, polymerase activity, and bodyweight gain were done using non-parametric Kruskal–Wallis and Mann–Whitney Wilcoxon tests with post-hoc Tukey tests. Survival durations were analyzed using log-rank Mantel–Cox test. Results were considered statistically significant at p value < 0.05. All analysis was done by GraphPad Prism software.

3. Results

3.1 Compatibility of European H9N2 and clade 2.3.4.4 H5N8 segments in reassortment

To assess the ability of A/turkey/Germany/R1685/2016 (H9N2) (designated H9N2) to reassort with HPAIV A/tufted duck/Germany/8444/2016 (H5N8) clade 2.3.4.4 subclade B (designated H5N8) in human-embryonic kidney 293T (HEK293T) cells, genome segments of H5N8 were replaced by single segments of H9N2 using reverse genetic systems in a 7 + 1 approach. All H9N2 segments, except PB1 and NP, yielded H5N8 infectious viruses indicating an incompatibility for exchanging these two segments (Fig. 1A). These results were confirmed in two different laboratories and using different rescue strategies. Conversely, H9N2 virus carrying H5N8 PB1 and/or NP segments were successfully rescued (data not shown). Reassortment of H5N8 with H9N2 M segment, however, produced only low progeny virus titers after propagation in eggs and, therefore, was not used for further characterization.

To further determine whether H9N2 segments generally show a restricted compatibility to reassort with HPAIV H5N8, segments of H5N8 were replaced by segments of G1-like A/chicken/Egypt/S12568C/2016 (H9N2) (designated H9N2-G1-like). Only the PB2 and PA of H9N2-G1-like yielded infectious H5N8 viruses and the rescue of a reassortant H5N8 virus with NS from H9N2-G1-like was not successful. Interestingly, NS1 proteins of H5N8 and H9N2-G1-like belong to allele A, while German H9N2 NS1 belongs to allele B (w). Moreover, swapping single segments of the current H5N8 virus with another HPAIV A/turkey/
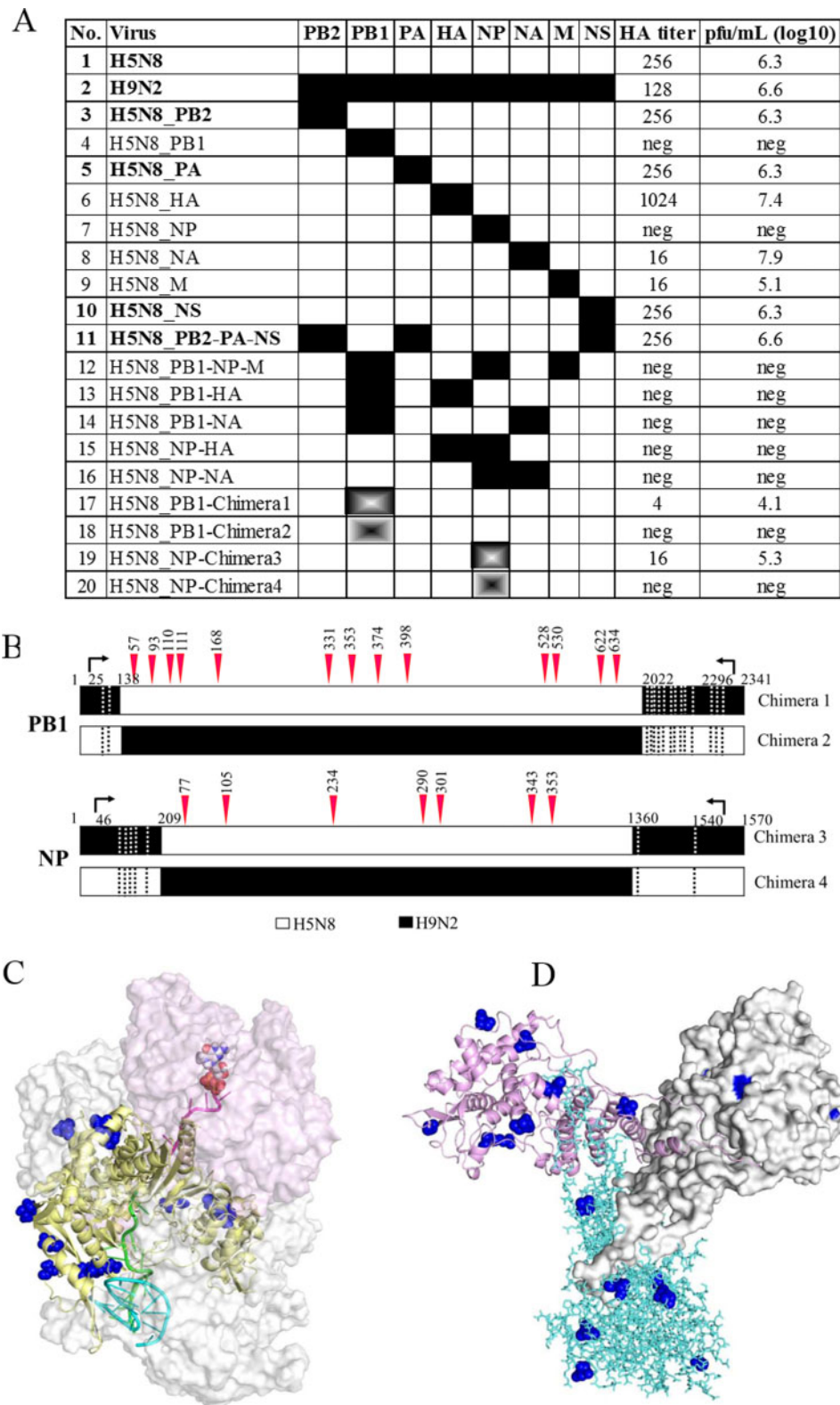
A

No.	Virus	PB2	PB1	PA	HA	NP	NA	M	NS	HA titer	pfu/mL (log10)
1	**H5N8**									256	6.3
2	**H9N2**	■	■	■	■	■	■	■	■	128	6.6
3	**H5N8_PB2**	■								256	6.3
4	H5N8_PB1		■							neg	neg
5	**H5N8_PA**			■						256	6.3
6	H5N8_HA				■					1024	7.4
7	H5N8_NP					■				neg	neg
8	H5N8_NA						■			16	7.9
9	H5N8_M							■		16	5.1
10	**H5N8_NS**								■	256	6.3
11	**H5N8_PB2-PA-NS**	■		■					■	256	6.6
12	H5N8_PB1-NP-M		■			■		■		neg	neg
13	H5N8_PB1-HA		■		■					neg	neg
14	H5N8_PB1-NA		■				■			neg	neg
15	H5N8_NP-HA				■	■				neg	neg
16	H5N8_NP-NA					■	■			neg	neg
17	H5N8_PB1-Chimera1		▨							4	4.1
18	H5N8_PB1-Chimera2		▨							neg	neg
19	H5N8_NP-Chimera3					▨				16	5.3
20	H5N8_NP-Chimera4					▨				neg	neg

Figure 1. Genetic compatibility of H5N8 and H9N2 viruses in this study. Results of H5N8 virus rescue after exchanging segments with European H9N2 virus showing hemagglutination (HA) titer and virus titers in plaque forming units (pfu/ml). neg = virus rescue was not successful (A). Chimera of PB1 and NP segments were generated by exchanging the non-coding regions at the 5′and 3′ends of H5N8 (white) and H9N2 (black). Silent mutations in these non-coding regions are shown as dotted lines while amino acid exchanges are shown in red triangles and the positions are written in black. The length of PB1 and NP was 2341 and 1570 nucleotides, respectively. Amino acid sequences were deduced from ORFs of PB1 (positions 25 to 2296) and NP (positions 46 to 1540). Numbering of the amino acids starts from the start codon (B). Tertiary structures of the H5N8-PB1 (yellow ribbons) interacting with PA and PB2 (C) and homotrimers of NP (D) were predicted using SWISS-Model. RNAs interacting with PB1 residues are shown in red, green, and cyan. Amino acid differences in the H5N8 PB1 and NP are shown as blue spheres.

Table 1. Genetic identity of different gene segments of H5N8 and H9N2 used in this study.

Segment	Number of nt differences (%)	Number of aa differences (%)	Positions (H9N2-x-H5N8)
PB2	188 (91.8%)	5 (99.3%)	I260V, R376K, D678F, V717A, N759K
PB1	119 (94.8%)	13 (98.3%)	M57T, S93A, T110A, V111M, K168R, D331E, R353K, A374T, E398D, A528T, V530I, C622G, Q634H
PA	117 (94.6%)	16 (97.8%)	L4F, A85T, V86M, D101E, K113R, E216D, A277S, L290F, I311M, P325L, I354V, G386D, V407I, K615R, D629E, I649L
NP	42 (97.2%)	7 (98.6%)	R77K, G105V, V234A, N290D, V301I, I343V, I353F
M1	40 (94.7%)	7 (97.2%)	A33V, R134K, F144L, M165I, V166A, K230R, R242K
M2	10 (96.6%)	5 (94.9%)	D13N, V28I, R45H, I51V, E66G
NS1	211 (69.6%)	76 (65.0%)	Too many to count
NS2	75 (79.5%)	24 (80.2%)	I6M, T7L, Q14M, V19M, E22G, V26E, E36G, R37S, R39K, I40L, S48T, A63G, T64K, N67E, E68Q, S70G, A81E, C83V, N85H, I86R, T88K, K89I, L100M, S111Q

nt, nucleotides; aa, amino acids.

Germany-MV/AR2487/2014 (H5N8) clade 2.3.4.4 subclade A (designated tk14) yielded infectious viruses (data not shown). This indicates that there are genetic incompatibilities for reassortment between H5N8 and H9N2 viruses used in this study.

To determine possible constraints for reassortment of H9N2 PB1 and NP with H5N8, we compared sequences between H5N8 and H9N2 segments (Table 1). Fifteen and seven silent nucleotide (nt) differences in the PB1 and NP, respectively, were observed in the non-coding regions (NCR), but no differences in the amino acid (aa) sequence (Fig. 1B and Table 1). Conversely, thirteen and seven non-synonymous differences were found in the respective open reading frame (ORF) (Fig. 1B). We therefore generated four chimeric PB1 and NP segments carrying exchanged NCRs from either H5N8 or H9N2 (Chimera 1: PB1$_{H5N8}$/NCRs$_{H9N2}$; Chimera 2: PB1$_{H9N2}$/NCRs$_{H5N8}$; Chimera 3: NP$_{H5N8}$/NCRs$_{H9N2}$; Chimera 4: NP$_{H9N2}$/NCRs$_{H5N8}$). Infectious H5N8 viruses were obtained only with PB1 or NP chimeras containing the ORFs from H5N8 (Chimeras 1 and 3) indicating that the NCRs of the different genomes do not affect functionality of the respective H5N8 genes (Fig. 1A and B). These results suggest that differences in the gene coding sequences and not in the packaging signal regions are responsible for the genetic incompatibility between H5N8 and H9N2 segments.

To achieve a better understanding of the possible effects caused by the aa differences between the H9N2 and H5N8 PB1 and NP proteins (Table 1), we superimposed the aa differences in the two H9N2 proteins onto the tertiary structure of the respective H5N8 proteins (Fig. 1C and D). The aa differences in the H5N8 PB1 are positioned in 'finger' or 'thumb' domains (Lo, Tang, and Shaw 2018). The aa differences in the H5N8 NP are highly variable among IAVs (Kukol and Hughes 2014) and are essential for NP-NP homo-oligomerization, PB2 binding and/or interaction with the tail loop (Ng, Wang, and Shaw 2009).

To study the impact of H9N2 segments on H5N8 fitness, we rescued six recombinant viruses: H5N8, H9N2, and H5N8 variants carrying H9N2 PB2 (H5N8_PB2), H9N2 PA (H5N8_PA), H9N2 NS (H5N8_NS), or H9N2 PB2, PA, and NS (H5N8_PB2-PA-NS). The replication of these viruses in two primary cell cultures (chicken embryo kidneys (CEK) and normal human bronchial epithelial cells (NHBE)) and two human cell lines (A549 and Calu-3 cells) was studied. Polymerase activity and interferon (IFN)-β response in A549 cells were determined. Furthermore, the impact of reassortment on H5N8 virulence, replication, IFN-β response, and T-cell activation in mice and virulence, excretion, tissue distribution, and transmission in chickens was studied.

3.2 Influence of H9N2 segments on H5N8 replication in CEK cells

CEK cells were infected at multiplicity of infection (MOI) of 0.01 for 1, 8, 12, 24, and 36 h at 37 °C. AIV H5N8 replicated to significantly higher levels than AIV H9N2 at each time point ($P < 0.003$) (Fig. 2A–D). Exchange of the PA and NS segments significantly increased replication of H5N8 at 8 hour post-infection (hpi) ($P < 0.0006$), while substitution of PB2 or all three segments had no effect ($P > 0.3$). At 12 and 36 hpi, all H5N8 reassortants replicated to similar levels as H5N8 virus ($P > 0.1$). At 24 hpi, H5N8_PB2-PA-NS replicated to slightly higher titers than H5N8 virus ($P = 0.045$) (Fig. 2A–D). Together, small differences in virus titers in CEK were only observed at 8 hpi for H5N8_PA and H5N8_NS and at 24 h for H5N8_PB2-PA-NS.

3.3 H9N2 NS segment alone or in combination with the PB2 and PA segments increased replication of H5N8 in NHBE cells

NHBE cells represent a good *ex vivo* model for studying IAV-infection of well-differentiated human primary airway cells with characteristics such as goblet and ciliated cells (Davis et al. 2015). NHBE cells were infected at an MOI of 0.01 for 1, 6, 12, 24, and 36 hpi at 37 °C. While H9N2 did not replicate on NHBE cells, the H5N8 replicated at moderate levels. Although H5N8_PB2 and H5N8_PA replicated at comparable levels as H5N8, H5N8_NS, and H5N8_PB2-PA-NS replicated to significantly higher titers ($P < 0.001$). Remarkably, replication of H5N8_PB2-PA-NS was observed earlier than other viruses (Fig. 2E–H). Taken together, H9N2 NS segment alone or in combination with the PB2 and PA segments increased replication of H5N8 in primary human bronchial epithelial cells.

3.4 H5N8 reassortants carrying either H9N2 NS or PB2, PA and NS gain significantly increased replication ability in human lung cells at lower respiratory tract temperature

Virus replication in human cells at 33 °C (e.g. upper respiratory tract temperature), 37 °C (e.g. lower respiratory tract
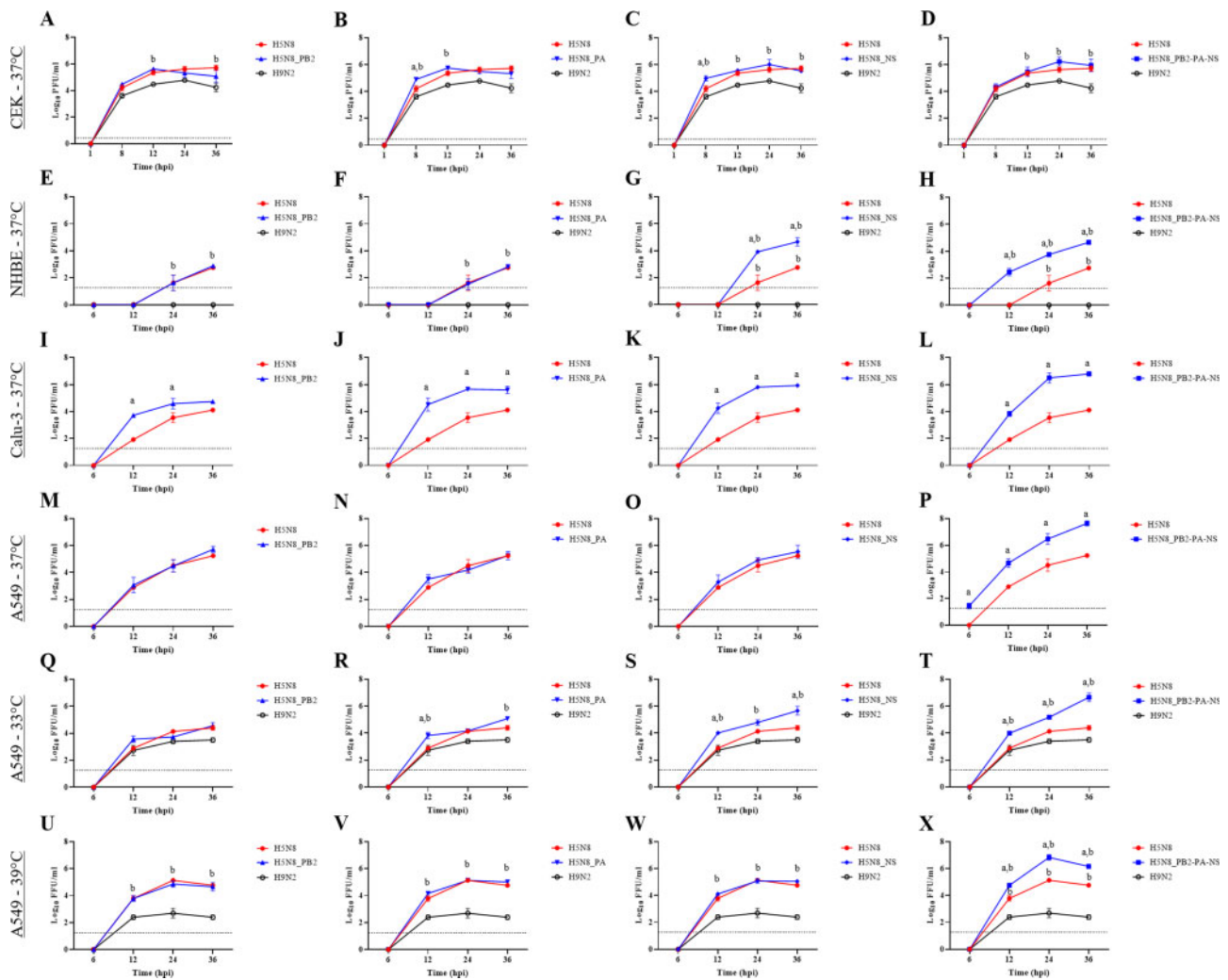
Figure 2. Replication of selected recombinant viruses in cells of avian or human origin. Replication of indicated viruses was analyzed in chicken embryo kidney cells (A–D), differentiated normal human bronchial epithelial cells (E–H), Calu-3 (I–L), and A549 (M–X) infected with an MOI of 0.01 for indicated time points. Significant differences compared to H5N8 and H9N2 viruses at P-value <0.05 are shown by letters 'a' and 'b', respectively. All cells were incubated after infection at 37 °C and additionally A549 cells were incubated at 33 °C (Q–T) or 39 °C (U–X). TPCK-trypsin was added for the replication of H9N2 in all cells, except NHBE cells. 0 values shown in the y-axis indicate no plaques or foci were detected in 400 μl or 50 μl per well, respectively. Dashed lines indicate the predicted low detection limit (LOD) of plaque and foci assays in this study (i.e. < 1 pfu/ffu in 400 μl or 50 μl, respectively).

temperature), and/or 39 °C (e.g. fever) was studied. Replication kinetics of recombinant viruses were compared in Calu-3 cells at 37 °C (Fig. 2I–L) and in A549 cells at 33 °C, 37 °C and 39 °C (Fig. 2M–X). At 37 °C, recombinant H5N8 replicated to only low titer compared to other reassortant H5N8 viruses in Calu-3 cells and virus progeny was first detected at 12 hpi and reached a maximum titer at 36 hpi (Fig. 2I–L). The replication of H5N8 increased significantly after reassortment with H9N2 PB2, PA, and/or NS (Fig. 2I–L). In A549 cells at 37 °C, the reassortment with PB2, PA, or NS segments independently did not affect the replication of the reassortant H5N8 (Fig. 2M–P). However, H5N8_PB2-PA-NS replicated earlier and exhibited significantly higher titers than other viruses (Fig. 2P).

In A549 cells, H5N8 virus replication was significantly higher at 39 °C than at 33 °C (P < 0.05) (Fig. 2Q–X), while H9N2 replicated at lower titers than H5N8 viruses particularly at 39 °C (Fig. 2Q–X). At 33 °C, the H5N8_NS demonstrated significantly higher titers at 12 and 36 hpi (Fig. 2S) and replication of H5N8_PB2-PA-NS was significantly higher than H5N8 at all periods (Fig. 2T). At 39 °C, H5N8_PB2-PA-NS replicated to higher levels compared to the

H5N8 virus (Fig. 2X). In summary, the combination of H9N2 PB2, PA, and NS segments significantly increased the replication of H5N8 in different human lung cells at different temperatures.

3.5 H9N2 PA reduced the polymerase activity of H5N8 at 33 °C and 39 °C, while PB2 only increased the polymerase activity at 39 °C

The impact of PB2 and PA on polymerase activity was assessed by a minigenome luciferase assay in HEK293T cells. The relative luciferase activity of the different minigenome compositions was compared to the wild-type H5N8 segments (Fig. 3A). At 33 °C, the activity of H9N2 polymerase was similar to that of H5N8, but greatly (75%) reduced at 39 °C. However, the H9N2 PB2 or PA combined with NP and the remaining polymerase subunits of H5N8 reduced the polymerase activity at 33 °C by 20 per cent (P < 0.001) (Fig. 3A). At 39 °C, the H9N2 PA resulted in a stronger reduction of the polymerase activity leading to a 55 per cent activity reduction compared to the wild-type H5N8 (P < 0.001). Conversely, H9N2 PB2 significantly increased (40%)
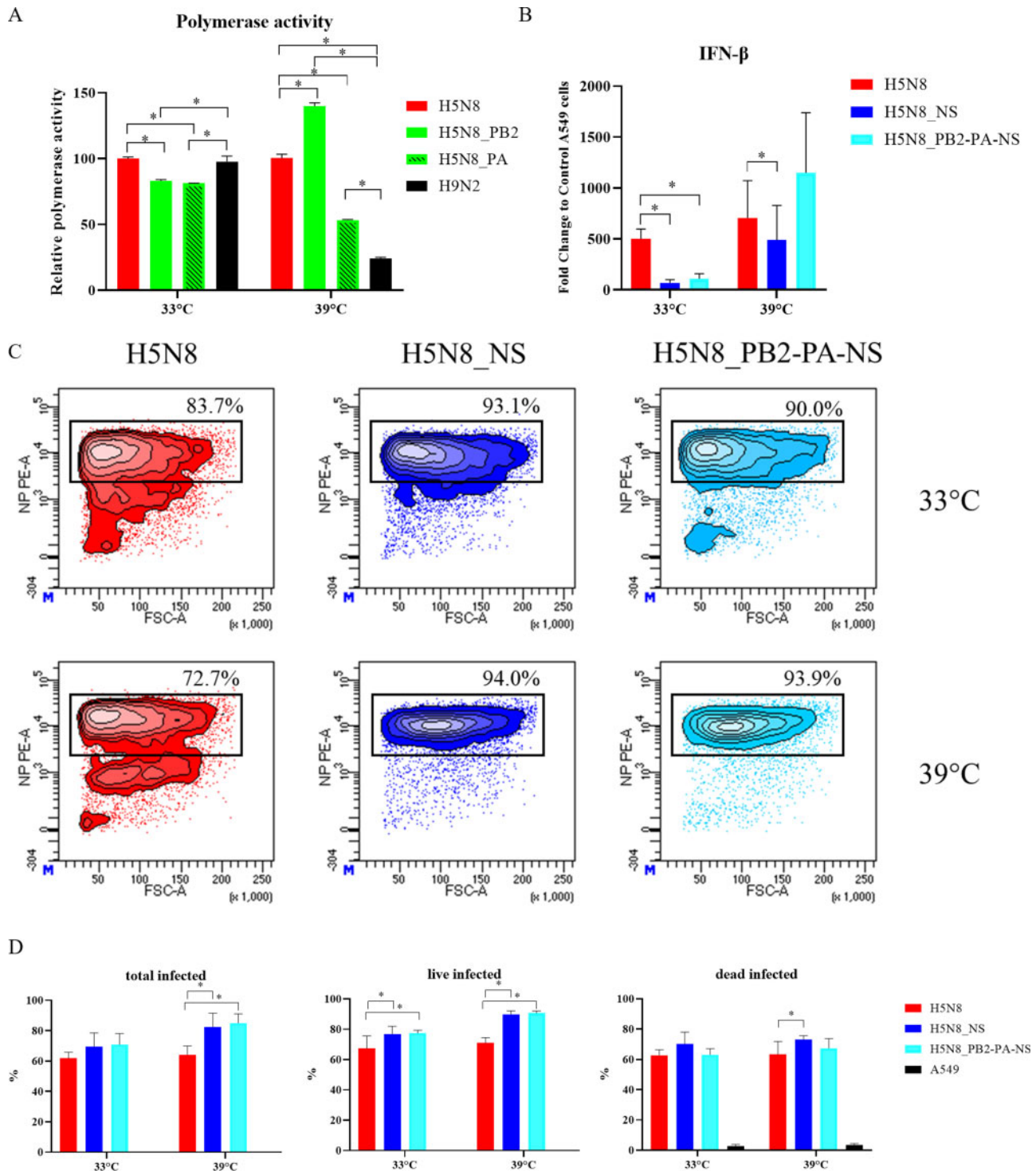
Figure 3. The impact of H9N2 segments on polymerase activity, interferon response, and number of infected A549 cells. Polymerase activity in human kidney embryonic cells (HEK293T) of indicated viruses normalized to the activity of H5N8 and expressed as x-fold change at 33 and 39 °C (A). Fold change induction of interferon-β in A549 cells of indicated viruses normalized to cells without infection inoculated with PBS at 33 °C or 39 °C (B). Representative results of flow cytometry after infection of A549 at MOI of 1 with H5N8 (red), H5N8_NS (dark blue), or H5N8_PB2-PA-NS (light blue) for 24 h at 33 °C (upper panel) or 39 °C (lower panel) (C). Infected, NP highly positive cells are given as percentages from total living cells based on uninfected control cells. The test was done in duplicates and repeated three times and results are shown as average and standard deviations of all replicates (D). Significant differences compared to H5N8 and H9N2 viruses at P-value <0.05 are shown.

the polymerase activity in combination with the other H5N8 NP and subunits at 39 °C (P < 0.001) (Fig. 3A). Generally, H9N2 PA and PB2 affected the polymerase activity of H5N8 in a temperature-dependent manner. While H9N2 PB2 supported higher polymerase activity of H5N8 at human lower respiratory tract temperature, PA significantly reduced the polymerase activity, which may explain the low activity of H9N2 at human lower respiratory tract temperature.

3.6 Compared to H5N8, the reassortant H5N8 carrying the H9N2 NS increased the IFN-*β* response in human A549 lung cells in a temperature-dependent manner

The amount of IFN-β gene expression was quantified via real-time reverse-transcription PCR (RT-qPCR) by amplification of mRNA of A549 cells 24 hpi with H5N8_NS or H5N8_PB2-PA-NS at either 33 °C or 39 °C. The results were normalized to the β-actin mRNA and expressed as x-fold change. The IFN-β response in H5N8 virus infected cells at 33 °C was 207-fold lower than the response at 39 °C (Fig. 3B). At 33 °C, the level of IFN-β gene expression in cells infected with H5N8_NS or H5N8_PB2-PA-NS was reduced compared to the H5N8 by 392- and 432-fold, respectively (Fig. 3B). Conversely, at 39 °C, H5N8_NS increased the IFN-β response by 441-fold compared to wild-type H5N8 infected cells and by 1,040-fold compared to cells infected with the reassortant H5N8_NS at 33 °C (Fig. 3B). Collectively, H9N2 NS inhibited IFN-β response of H5N8 at human upper respiratory tract temperature and increased IFN-β response at lower respiratory tract temperature.

3.7 Compared to H5N8, the reassortant H5N8 carrying the H9N2 NS significantly infected higher number of human A549 lung cells

To test whether the number of infected cells correlate with the pattern for IFN-β response, A549 cells were infected at MOI of 1 for 24 h with H5N8, H5N8_NS, or H5N8_PB2-PA-NS at either 33 °C or 39 °C (Fig. 3C and D). The total number of cells as well as the number of viable or dead cells infected with different viruses were calculated using flow cytometry and standard anti-NP-antibodies (Fig. 3C and D). The results showed that the total number of cells and the number of viable cells infected with H5N8 was slightly higher, although not statistically significant, at 39 °C than at 33 °C ($P > 0.4$). Conversely, the total number and number of viable cells infected with H5N8_NS or H5N8_PB2-PA-NS was higher at 39 °C than at 33 °C ($P < 0.03$). The total number of cells infected with H5N8_NS or H5N8_PB2-PA-NS was higher than H5N8 at 33 °C and 39 °C although statistical differences were only observed at 39 °C ($P < 0.0003$). The number of viable cells infected with H5N8_NS or H5N8_PB2-PA-NS was significantly higher than H5N8 at 33 °C and 39 °C ($P < 0.01$). There were no statistical differences between the number of cells infected with H5N8_NS or H5N8_PB2-PA-NS at both temperatures ($P \geq 0.1$). The number of dead cells was significantly higher after the infection with H5N8_NS than H5N8 at 39 °C ($P < 0.02$). Altogether, H9N2 NS significantly increased the number of live infected cells, which is partially correlated with the inhibition of IFN-β response particularly at the human upper respiratory tract temperature.

3.8 H5N8 reassortants carrying the H9N2 PB2, PA or NS alone or in combination demonstrated increased virulence in mice as indicated by rapid onset of mortality

Mice inoculated intra-nasally with 10^5 plaque forming units (pfu) (high dose) (Fig. 4A) or 10^3 pfu (low dose) of each virus (Fig. 4B) were observed for 11 days and the mean time to death (MTD) was calculated. Four days after high dose inoculation only two mice infected with H9N2 had to be sacrificed because of drastic (>25%) body weight (BW) reduction (Fig. 4A). Mice infected with H5N8 virus died between 3 and 6 dpi with MTD of 4.1 days (Fig. 4A) similar to mice infected with reassortant H5N8 carrying segments from H9N2 that died within 4 dpi. Mice

infected at high dose with H5N8_PB2 started to die at 1 dpi with MTD of 2.8 days. In the groups infected with H5N8_PA, H5N8_NS, and H5N8_PB2-PA-NS mice started to die at day 3 and the MTD values were estimated to be 3.2, 3.5, and 3.5 days, respectively (Fig. 4A). The survival durations of H5N8_PB2 and H5N8_PA inoculated mice were significantly shorter than those inoculated with H5N8 ($P < 0.008$). None of the mice in the sterile medium-inoculated group (sham group) died. After low dose inoculation, all mice inoculated with H9N2 survived. Mice infected with H5N8 virus died within 9 dpi with MTD of 7.2 days (Fig. 4B). Mortality started at day 5 in groups of mice inoculated with H5N8_PB2 and H5N8_PB2-PA-NS and 6 dpi in groups of mice inoculated with H5N8_NS or H5N8_PA with MTD values of 6.2, 7, 7.2, and 5.6 days, respectively (Fig. 4B). Mice inoculated with H5N8_PB2-PA-NS exhibited significantly shorter survival duration than H5N8-inoculated mice ($P < 0.013$). Taken together, H9N2 segments increased virulence of H5N8 in mice as indicated by rapid onset of mortality and short survival durations.

3.9 The impact of reassortment of H5N8 with H9N2 on body weight of inoculated mice

After high dose inoculation, animals showed reduction in BW at 1 dpi compared to the relative BW immediately before infection and compared to the control group (Fig. 4C). H9N2 inoculated mice exhibited a transient reduction in BW at 2 and 3 dpi and the BW started to increase at 4 dpi to the end of the experiment, although at significantly lower levels than the control group ($P < 0.01$) (Fig. 4C). Mice inoculated with H5N8 viruses showed drastic reduction in BW until the day of death or killing and the reduction in BW gain was statistically significant compared to the sham and H9N2-inoculated groups ($P < 0.001$). Compared to H5N8, significant reduction in BW was observed in H5N8_NS inoculated mice at 1–3 dpi ($P < 0.0002$), in H5N8_PA and H5N8_PB2 inoculated mice at 1 and 3 dpi ($P < 0.0001$) and in H5N8_PB2-PA-NS at 2 dpi ($P < 0.001$) (Fig. 4C). After low dose inoculation, H9N2 had no effect on the BW, while H5N8 viruses caused significant reduction in BW of inoculated mice. The reassortment with H9N2 PA or NS did not significantly alter the impact of H5N8 on BW. However, H5N8_PB2 and H5N8_PB2-PA-NS viruses at 3–5 dpi and 2–5 dpi, respectively caused significant increased reduction in the BW compared to the wild-type H5N8 virus ($P < 0.001$) (Fig. 4D). These results indicate a specific impact of the H9N2 PB2, PA, and NS segments particularly when combined in BW loss after infection with H5N8.

3.10 Reassortment of H5N8 with H9N2 did not lead to significant increase of viral titers in the lungs of infected mice

The titer of viruses in the lungs, brain, and spleen homogenates from humanely killed or deceased high-dose inoculated mice at 3 dpi was determined by plaque test in MDCKII (Fig. 4E). Viruses were recovered from the lungs of all inoculated mice at comparable titers (~10^4 PFU/g) and there was no significant difference in viral titers between different groups (Fig. 4E). Infectious virus was detected in the brain of H5N8-inoculated mice (~$10^{3.3}$ PFU/g), H5N8_PB2 (~$10^{2.0}$ PFU/g), and H5N8_PA (~$10^{2.0}$ PFU/g) only (data not shown). No infectious virus was detected in the spleen of any mouse. Generally, H9N2 PB2, PA, or NS segments did not significantly increase H5N8 load in the lungs of infected mice.
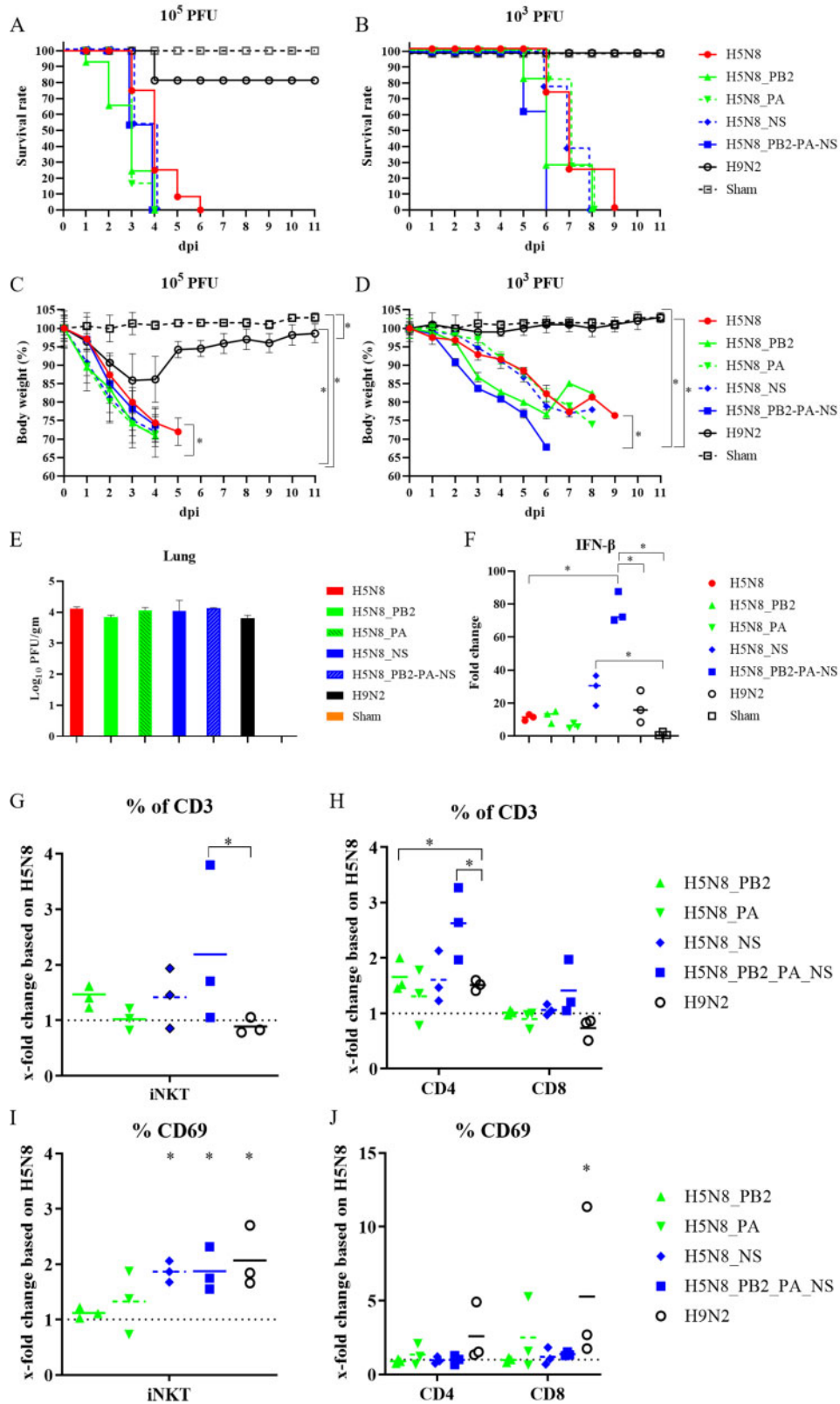
Figure 4. The impact of H9N2 PB2, PA, and NS segments on viral fitness of reassortant H5N8 in mice. Mortality and BW loss after intra-nasally high dose inoculation (10^5 pfu/mouse) (A, C) or with low dose 10^3 pfu/mouse (B, D). Mice that lost more than 25 per cent of BW at day 3 were humanely killed after deep anesthesia by Isoflurane and cervical dislocation. Significant differences compared to mice inoculated with H5N8, H9N2, or sham group at P-value <0.05 are shown (C, D). Viral titers in lung samples obtained from high-dose inoculated mice were determined by plaque assay in MDCKII and expressed as plaque forming unit per gram (PFU/gm). (E). Results of IFN-β expression in the lungs of high-dose inoculated mice at 3 dpi ($n = 3$). Fold change of IFN-β mRNA was normalized to sham mice shown as individual and average values (F). T-cell frequencies and activation in the spleen of high-dose inoculated mice ($n = 3$) at 3 dpi. Frequency of iNKT cells and CD4+ and CD8+ T-cells among CD3+ cells (G, H) and frequency of CD69+ iNKT cells (I). Asterisks in panels I and J refer to significant differences compared to H5N8. Results were normalized to H5N8-inoculated mice with 10^5 pfu.

3.11 H9N2 NS alone or in combination with PB2 and PA significantly increased IFN-β response in the lungs of infected mice

IFN-β mRNA in the lungs of high-dose inoculated mice at 3 dpi was quantified and normalized to the β-actin mRNA for each sample (Fig. 4F) (Livak and Schmittgen 2001). H5N8_PB2-PA-NS and H5N8_NS increased the expression of IFN-β by 59- and 22-fold, respectively. H9N2 infection increased the IFN-β response by 13-fold, while the recombinant wild-type H5N8 and H5N8_PB2 mounted an IFN-β activation at similar levels, ∼9-fold. H5N8_PA was slightly less efficient to induce IFN-β response compared to other viruses, although H5N8_PA inoculated mice expressed IFN-β at 5-fold higher than the control group (Fig. 4F). These results indicate that H9N2 segments particularly NS affected IFN-β response in the lungs of H5N8-infected mice.

3.12 Reassortment with H9N2 activated iNKT cells in the spleen of inoculated mice in a dose-dependent manner

To get an insight into the impact of H5N8 reassortment with H9N2 on T-cell response using flow cytometry analysis, spleen samples were collected from mice at 3 dpi. Results were normalized to the H5N8 response after subtraction of values from the control group (Fig. 4G–J). High dose inoculation with H5N8_PB2-PA-NS resulted in increased frequencies of iNKT, CD4+, and CD8+ cells among CD3+ lymphocytes in the spleen compared to the wild-type H5N8 infected mice. Interestingly, H5N8_NS and H5N8_PB2-PA-NS significantly activated iNKT cells, measured by CD69 expression, in the same amount as the H9N2 control and in contrast to wild-type H5N8. Activation of classical CD4+ and CD8+ T cells failed after infection with these viruses (Fig. 4G–J). Inoculation of mice with 10^3 pfu H9N2 did not significantly affect the stimulation of iNKT cells compared to the control group (data not shown). Altogether, H9N2 NS increased activation of early responding iNKT cells in the spleen after infection with high dose of H5N8 virus.

3.13 In chickens, reassortment with H9N2 NS had a negative impact on chicken-to-chicken transmission

Ten chickens were inoculated oculonasally and five contact chickens were added 1 dpi to each group. Birds were observed for 10 dpi. The pathogenicity index (PI) based on the daily clinical scoring for each bird ranging from 0 (avirulent) to 3 (highly virulent) and MTD were calculated. All H9N2-inoculated birds survived without showing clinical signs. All H5N8 inoculated birds died within 2 days (H5N8_NS, H5N8_PB2-PA-NS, and H5N8 inoculated chickens) or 3 days (H5N8_PB2 and H5N8_PA inoculated chickens) with comparable PI values of 2.7 and MTD of 2.8 (H5N8_PB2), 2.2 (H5N8_PA), or 2.0 (H5N8_NS, H5N8_PB2-PA-NS, and H5N8) (Fig. 5A). Contact birds to chickens inoculated with H9N2, H5N8_NS or H5N8_PB2-PA-NS did not show any clinical signs and remained healthy. All contact birds to chickens inoculated with H5N8 and H5N8_PB2 died with MTD of 4 and 7.6 dpi (3 and 6.6 days post contact). Only 3/5 contact chickens to chickens inoculated with H5N8_PA died with MTD of 4.7 dpi (3.7 days post contact) (Fig. 5B) and the two remaining birds did not exhibit any clinical signs. The survival durations of contact chickens to H5N8_PB2 and H5N8_PA-inoculated chickens were significantly longer than that of chickens cohoused with H5N8-inoculated chickens ($P < 0.002$). These results indicate that the reassortment with H9N2, particularly H9N2 NS segment, reduced bird-to-bird transmission of H5N8 virus without significant impact on virulence in inoculated chickens.

Virus excretion was determined in oropharyngeal (OP) and cloacal (CL) swabs and different organs 2 dpi by plaque assay in MDCKII cells. The results are expressed as plaque forming units per ml (PFU/ml) (Fig. 5C). The titers of all H5N8 viruses in inoculated chickens were comparable ($P > 0.1$). H9N2 was not recovered from any chicken although all inoculated chickens seroconverted, while H5N8 viruses were excreted at higher levels from the cloaca than the oropharynx. All H5N8-inoculated chickens died within 3 dpi and, therefore, no swabs were taken at 4 dpi. No infectious virus was obtained from contact chickens after titration of samples using plaque test at any time point and all surviving contact chickens were negative for anti-NP antibodies. However, viral RNA was detected in 4/5 and 3/5 chickens co-housed with chickens inoculated with H5N8_PB2 or H5N8_PA at 4 dpi, respectively (data not shown). These results indicate that the reassortment with H9N2 NS segment reduced the excretion of H5N8 viruses to undetectable limits in contact chickens.

Replication and viral tissue tropism were compared at 2 dpi in chickens inoculated with H5N8, H5N8_NS, or H5N8_PB2-PA-NS by plaque test (Fig. 6), histopathology, and immunohistochemistry (Table 2 and Supplementary Fig. S1). Compared to H5N8, the titer of infectious viruses in organs of inoculated chickens was generally reduced after inoculation with H5N8_NS and to lesser extent with H5N8_PB2-PA-NS (Fig. 6). H5N8 yielded the highest tissue necrosis score and most abundant viral antigen distribution, followed by H5N8_NS and least H5N8_PB2-PA-NS (Table 2 and Supplementary Fig. S1). Differences in necrosis scores were most obvious in duodenum, liver, and thymus, and for antigen distribution in liver, kidney, and thymus (Table 2). In the lung and heart, antigen distribution and necrosis did not differ significantly between groups. In particular, H5N8 was associated with a ubiquitous endotheliotropism that was markedly restricted after H5N8_NS and even more after H5N8_PB2-PA-NS infection, particularly in the liver, kidney, pancreas, and gastrointestinal tract (Table 2 and Supplementary Fig. S1). Together, the results from the chicken experiments indicate that the reassortment of H5N8 virus particularly with H9N2 NS segment has a negative impact on transmission and virus excretion in contact chickens.

4. Discussion

Although AIV H9N2 was the donor of non-HA/NA segments for AIV, which were highly virulent in humans (Guan et al. 1999; Fusaro et al. 2011; Pu et al. 2015), there are no published data for natural reassortment of the internal genes of H9N2 with H5N8, since 2016 so far. Here, we analyzed the compatibility of two recent German H9N2 and H5N8 clade 2.3.4.4 viruses to reassort and studied the impact of reassortment on H5N8 fitness *in vitro* and *in vivo*. Only the H9N2 PB2, PA, and NS segments resulted in infectious reassortant H5N8 viruses with high titers, while H9N2 PB1 and NP were not compatible with productive replication of the other H5N8 segments used in this study. It is worth mentioning that the adaptation of AIV in specific hosts (wild vs. domestic birds) may affect the range of reassortment between H5N8 and H9N2 in this study (Lu, Lycett, and Leigh Brown 2014). While H9N2 viruses can circulate undetected in poultry, HPAIV-infected poultry are usually culled (Alexander 2000). Therefore, some H9N2-AIV may adapt to domestic birds, while the unprecedented incursions of H5N8 into poultry worldwide was mostly via separate direct or indirect contact at the wildlife-domestic
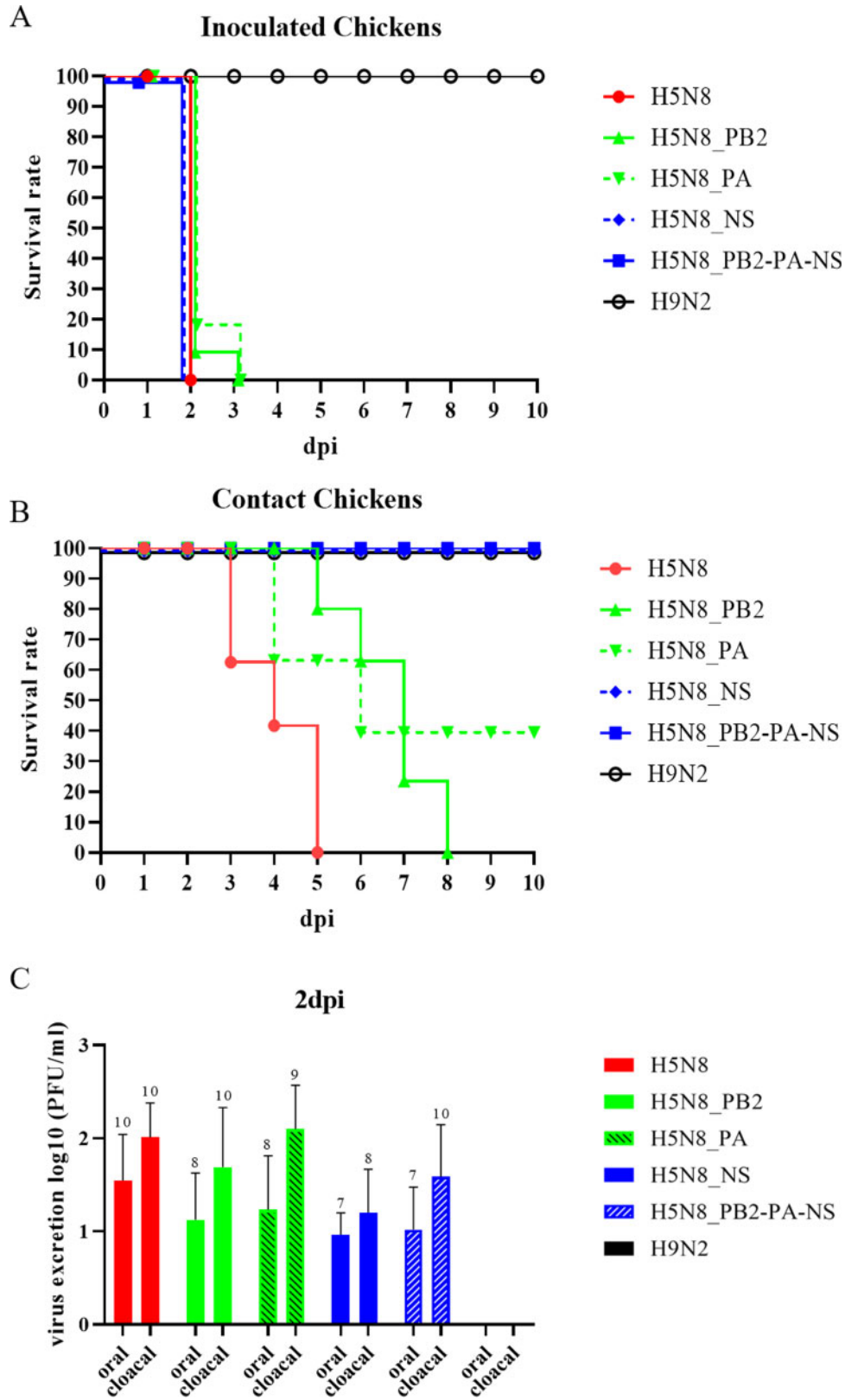
Figure 5. The impact of H9N2 PB2, PA, and NS on H5N8 virus fitness in chickens. Survival rate of chickens inoculated with different viruses via oculonasal route (A) and survival rate of contact chickens (B). Virus excretion at 2 dpi from inoculated chickens was determined using plaque test in MDCKII. Numbers refer to number of chickens tested positive out of 10 inoculated chickens (C).
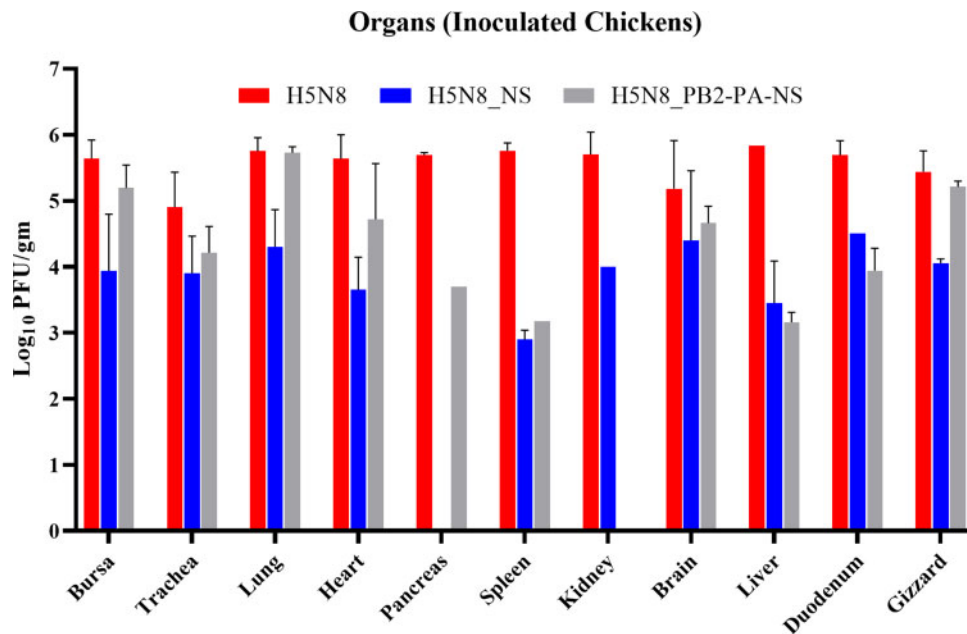
Organs (Inoculated Chickens)

Figure 6. The impact of H9N2 PB2, PA, and NS on H5N8 virus replication in chicken organs. Viral titers in different organs of inoculated-chickens at 2 dpi were determined using plaque test in MDCKII cells. Results are shown as average and standard deviation of positive samples.

animal interface with limited lateral spread in poultry holdings (Mulatti et al. 2018; Poen et al. 2018; Pohlmann et al. 2018). Furthermore, the reassortment of H5 clade 2.3.4.4 yielding diverse H5Nx viruses occurred mainly via exchange of the NA segment and it occurred mostly in wild birds (Lee et al. 2017). Recently, the isolation of reassortant H5N2 viruses from poultry in Egypt, where both H5N8- and H9N2-AIV are endemic, has been described in farmed broilers and ducks after obtaining the H9N2 NA or H5N8 HA segments (Hagag et al. 2019; Hassan et al. 2020). No evidence is available for reassortment of internal segments. Interestingly, H5N8 detected in wild birds in Germany in 2016/2017 were found to possess varying PB1 segments and the evolution of H5N5 was associated with acquisition of novel PB1 and NP segments (Pohlmann et al. 2018). Findings of this study may explain this variation of PB1 and NP during the introduction of H5N8 in Europe in 2016/2017.

Reassortment may be limited due to RNA–RNA, RNA–protein or protein–protein interaction constrains (Lowen 2017). Along this line, it has recently been reported that RNA packaging signal regions restrict reassortment of human H3N2 and avian H5N8 and H7N9 viruses (White et al. 2019). Another study showed that the interaction of RNA with specific NP amino acids governed the successful reassortment of bat H17N10 and seal H7N7 viruses in mammalian cells (Moreira et al. 2016; Bolte et al. 2019). In the current study, H9N2 PB1 and NP were not compatible with the other H5N8 proteins although they were more similar on the nucleotide level than the compatible PB2, PA, and NS segments. Intriguingly, this incompatibility was due to differences in the ORF and not in the packaging region and was not associated with HA and/or NA genes as previously observed (White et al. 2019). Therefore, it is tempting to assume that incompatibility of H5N8 and H9N2 segments occurs possibly on the protein–protein interaction level, which remains to be investigated. No data are available so far on the biological function of these peculiar H5N8 PB1 and NP differences, which merit further investigation.

The efficient influenza virus replication, including H9N2, in mammalian cells via increased replication speed or decreased sensitivity to antiviral effectors can be strain specific (Kurokawa et al. 1999; Grimm et al. 2007; Dittmann et al. 2008). Compared to some Asian H9N2 viruses (SJCEIRS-H9-Working-Group 2013), H9N2 virus in this study did not replicate efficiently in human cells probably due to high adaptation to birds conferred by the HA (e.g. receptor binding). Despite limitations for H5N8/H9N2 reassortment, findings in the current study provide strong evidence that H9N2 internal segments can increase the replication of H5N8 virus in mammalian cells as recently described for some Egyptian H5N1/H9N2 reassortants (Arai et al. 2019). Although H9N2 segments had minor effect on virus replication in primary chicken cells, the synergism between H9N2 PB2, PA, and NS resulted in significant high replication of H5N8 in all human cells used in this study independent of temperature. Nevertheless, different replication levels of H5N8/H9N2 reassortants were observed in NHBE, A549, and Calu-3, which is in line with variable replication of some influenza viruses in these cells in other studies (Gerlach et al. 2013; Kanrai et al. 2016). Although it remains to be identified, this variation in replication of H5N8/H9N2 reassortants in different cells may be attributed to some cellular and viral factors. NHBE cells are a pseudostratified primary differentiated bronchial epithelial cell culture containing ciliated and non-ciliated cells and are more closely related to the *in-vivo* situation. Calu-3 cells are a bronchial epithelial adenocarcinoma cell line isolated from a 25-year-old Caucasian male, while A549 cells are thought to be a type II alveolar epithelial cell line isolated from a human pulmonary adenocarcinoma (Papazian, Würtzen, and Hansen 2016). Calu-3 and NHBE cells are airway epithelial cells; however, in Calu-3 each H9N2 segment increased H5N8 replication, while in NHBE cells only H9N2 NS segment had a significant impact on multiple-cycle replication of H5N8.

An obvious shortcoming here is that we did not measure IFN-β expression in different cell cultures after the infection

Table 2. Histopathology and tissue tropism in chickens.

	Cell tropism and necrosis score	H5N8_NS		H5N8_PB2-PA-NS		H5N8	
		Max score[a]	Group score[b]	Max score[a]	Group score[b]	Max score[a]	Group score[b]
Lung	Endothelium	+++	6	+++	8	+++	9
	Respiratory epithelium	++	6	+++	7	+++	8
	Necrosis score	+++	7	+++	9	+++	9
Heart	Endothelium	++	4	+	3	+++	8
	Myocardium	++	6	++	6	++	6
	Necrosis score	++	4	++	5	++	4
Proventriculus	Endothelium	++	4	+++	7	+++	9
	Mucosal / glandular epithelium	++	5	++	6	+++	7
	Necrosis score	+	2	+	3	++	5
Gizzard	Endothelium	+++	3	+++	n.c.[c]	+++	n.c.[c]
	Mucosal epithelium	+	2	+	n.c.[c]	++	n.c.[c]
	Necrosis score	+	2	+	n.c.[c]	+	n.c.[c]
Duodenum	Endothelium	+++	4	++	4	+++	9
	Mucosal epithelium	0	0	+	1	++	5
	Necrosis score	0	0	0	0	+	2
Cecum	Endothelium	++	3	++	4	+++	9
	Mucosal epithelium	++	3	++	2	++	4
	Necrosis score	+	1	++	2	++	3
Cecal tonsil	Endothelium	+	2	+	3	+++	9
	Immune cells	+	1	+	2	++	5
	Necrosis score	++	6	++	6	+++	9
Pancreas	Endothelium	++	2	0	0	+++	8
	Parenchymal epithelium	+	2	+	1	+	3
	Necrosis score	0	0	+	1	+	2
Liver	Endothelium	+	1	+	1	+++	9
	Parenchymal epithelium	+	1	++	4	++	6
	Necrosis score	+	2	+	2	++	6
Kidney	Endothelium	+	2	+	1	+++	9
	Parenchymal epithelium	+	2	+	1	++	4
	Necrosis score	+	1	+	1	++	5
Spleen	Endothelium	++	n.c.[c]	++	4	+++	n.c.[c]
	Immune cells	++	n.c.[c]	++	6	++	n.c.[c]
	Necrosis score	++	n.c.[c]	+++	9	+++	n.c.[c]
Bursa	Endothelium	++	4	++	6	+++	9
	Mucosal epithelium	0	0	0	0	0	0
	Immune cells	+	3	+	3	++	5
	Necrosis score	++	4	+	3	++	6
Thymus	Endothelium	++	5	++	6	+++	9
	Immune cells	++	5	+++	8	+++	9
	Necrosis score	++	5	+++	7	+++	8
Brain	Endothelium	++	3	+++	6	+++	9
	Neurons, glia, epithelium	++	5	++	3	++	6
	Necrosis score	++	4	++	3	++	6

Necrosis scoring and detection of viral antigen in chickens infected with H5N8_NS, H5N8_PB2-PA-NS, or H5N8, three animals per group. Necrosis scoring on a scale 0 to 3+: 0 = no lesion, 1+ = mild, 2+ = moderate, 3+ = severe. Antigen detection on a labeling scale 0 to 3: 0 = negative, 1+ = focal to oligofocal, 2+ = multifocal, 3+ = coalescing foci or diffuse labeling.
[a]Max score: maximum of tissue score reached in this group.
[b]Group score, sum of '+' in this group.
[c]n.c.: not calculated, not all tissues present for evaluation.

with different H5N8/H9N2 reassortants to elucidate the role of PB2 and PA in the inhibition of IFN-response (Hayashi, MacDonald, and Takimoto 2015a; Gao et al. 2019) or to quantify IFN-β levels in different cells (Hsu et al. 2012). Nevertheless, our results revealed that H5N8 viruses carrying H9N2 NS was more efficient to inhibit IFN-β response, which was correlated with the increased number of live infected cells. Therefore, it is likely that after the infection of NHBE cells with H5N8_PB2 or H5N8_PA H5N8 NS was not as efficient as H9N2 NS to block the IFN-β response or the number of infected cells was too low to support high virus replication and thus increased IFN-β-inhibition. Conversely, in Calu-3 H9N2 PA and to lesser extent PB2 increased the replication of H5N8. The differentiated NHBE cells differ physiologically from the monoculture cells (e.g. Calu-3 or A549) in mucin secretion, receptor distribution, proteases, and IFN-β response and the replication of different influenza viruses may vary in different cells of the human respiratory tract (Matrosovich et al. 2004; Chan et al. 2010; Kreft et al. 2015; Gerlach et al. 2017). Moreover, PB2 and PA play a role in the inhibition of innate immune response (e.g. IFN-β) (Graef et al. 2010; Zhao et al. 2014; Hayashi, MacDonald, and Takimoto 2015a; Gao et al. 2019), and synergism with NS1 is required for efficient virus replication *in vivo* and *in vitro* (Varga et al. 2011; Nogales et al. 2017). It is worth mentioning that NS1 inhibit the innate immune response mostly by shutoff-active host IFN-related mRNAs and cytokine release, while PA-x preferentially degrades genes associated with cellular protein metabolism and protein repair (Chaimayo et al. 2018). Therefore, it is plausible that H9N2 PB2 or PA, through different cell-dependent pathways than by NS1, may inhibit the innate immune responses in Calu-3 cells. Furthermore, it is reasonable to suggest that higher replication of H5N8_PB2 in Calu-3 is also attributed to the higher polymerase activity conferred by PB2 at high temperature as previously described (Bradel-Tretheway et al. 2008). Although H9N2 NS significantly reduced IFN-β response and increased the number of H5N8-infected alveolar epithelial cells (i.e. A549) at different temperature, it was astonishing that single H9N2 did not increase H5N8 replication at high temperature. Surprisingly, data on the underlying mechanism for variable susceptibility of Calu-3 and A549 to influenza viruses are scarce, although both cell lines are commonly used in influenza virus research. Calu-3 and A549 are different cell lines and they vary physiologically with different cell internalization and trafficking pathways (Capel et al. 2016; Papazian, Würtzen, and Hansen 2016; Lujan et al. 2019). Efficient replication of some influenza viruses in Calu-3 than in A549 was attributed to such physiological variations (e.g. to proteolytic enzymes (Böttcher et al. 2006; Bottcher-Friebertshauser et al. 2011)). The impact of H9N2 PB2, PA, and NS on different steps of virus replication in Calu-3 and A549 and interaction with cellular factors should be further investigated.

Another notion was that H5N8_PB2-PA-NS had higher IFN-β response at 39 °C, although not statistically significant, compared to H5N8. It should not be totally excluded that some influenza viruses can replicate at high levels despite the high interferon response (Penski et al. 2011; Petersen et al. 2018). Moreover, this relative inefficiency to block the IFN-β response can be probably compensated by the higher and early replication (Kurokawa et al. 1999) and/or higher polymerase activity conferred by PB2 at high temperature. Although at 33 °C the activity of H9N2 was similar to that of H5N8, H9N2 PB2, and PA reduced the polymerase activity of H5N8. Conversely, at 39 °C compared to H5N8, H9N2 exhibited significantly lower polymerase activity, which is mostly driven by the H9N2 PA. Recently,

lower polymerase activity conferred by PA has been shown to drive the acquisition of mammal-adaptation markers in H7N9 PB2 (i.e. E627K) (Liang et al. 2019), known to increase polymerase activity in mammals. It has been recently shown that H5N8 viruses from 2016 to 2017 outbreak had a lower polymerase complex activity in human cells with minor impact on virus replication in cell culture (Vigeveno et al. 2020). This low polymerase activity was markedly increased with either the PB2 or PA of an H5N8 from 2014 to outbreak (Vigeveno et al. 2020). Similarly, PA of the pandemic-H1N1/2009 enhanced polymerase activity of chicken-origin H3N2 in mammalian cells at 37 °C, but not at the lower temperature of 34 °C (Bussey et al. 2011), which was restored by reassortment with PB2 (Hayashi et al. 2015b). Therefore, H9N2 PB2 and PA may balance the replication of the virus in human cells at different temperatures (i.e. in upper vs. lower respiratory tracts). It is worth mentioning that polymerase activity does not always correlate with the level of replication of influenza viruses in cell culture (Chin et al. 2014).

Previous studies showed the high compatibility of H5N1 and H9N2 for reassortment and increased virulence of reassortant H5N1 viruses in mammals after acquisition of H9N2 PB2, PA, NP, and/or NS (Hao et al. 2016; Arai et al. 2019). In the current study, H9N2 exhibited low virulence in mice. Conversely, H5N8 killed all mice inoculated with low or high dose and reassortment of H5N8 with H9N2 segments, particularly PB2, increased virus virulence as indicated by rapid onset of mortality, shorter MTD, and higher BW loss. PB2 was also associated with high virulence observed for some H5Nx in mice (Park et al. 2015; Wang et al. 2017). The interplay of NS1 with the immune system and the impact on mortality is well known. Here, H9N2 NS alone or in combination with PB2 and PA was not as efficient as the respective H5N8 segments to inhibit IFN-β or T-cell immune responses in lungs of infected mice. H5N8 NS in this study belongs to allele A, while H9N2 NS belongs to allele B, which blocked the IFN-β response less efficiently than allele A NS at 37 °C (Zohari et al. 2010). However, the ability of H9N2 NS to inhibit innate immune response in the upper respiratory tract as seen in A549 at 33 °C may support virus replication at early stage of infection. Conversely, H9N2 NS was not efficient to inhibit the IFN-β response at 39 °C (Szretter et al. 2009). Furthermore, an elevated IFN-β expression was mostly accompanied by an increased activation of early responding iNKT cells, which are able to improve the outcome of influenza virus infections (Kok et al. 2012) by mediating efficient NK and CD8+ T cell activation (Ishikawa et al. 2010). However, the infection exacerbated too fast to mount specific antiviral responses.

The reassortment between H5N8 and H9N2 segments did not affect virulence or early excretion of H5N8 in inoculated chickens. Strikingly, the reassortment with H9N2, particularly with the H9N2 NS segment, had a strong impact on chicken-to-chicken transmission as indicated by extended MTD or lack of morbidity, mortality, and virus excretion in contact birds. The impact of the NS segment was also previously demonstrated by our groups and others showing that the NS segment was important for virus replication and endotheliotropism of H7N1 in chickens (Abdelwhab el et al. 2016), virulence of H5N1 and transmission in chickens and/or mice (Li et al. 2006; Jiao et al. 2008), and increased replication of AIV and swine influenza viruses in mammalian cells (Kanrai et al. 2016; Petersen et al. 2018). Moreover, a recent study has shown that a Chinese H9N2 PB2 segment enhanced the fitness of H5N1 and H5N8 from earlier 2.3 clades in chickens (Hao et al. 2019), even though they are genetically different compared to the recent H5N8 clade 2.3.4.4b viruses.

In conclusion, findings of this study showed that the two recent European H9N2 and H5N8-clade 2.3.4.4b viruses used in this study had restricted compatibility for reassortment due to mutations outside the packing region. Although reassortment with H9N2 increased replication of H5N8 in human cells, it had a detrimental effect on transmission in chickens. This study is important for zoonotic risk assessment after reassortment of contemporary H5N8 and H9N2 AIV similar to those used in this study. Nevertheless, findings in this study might indicate the potential of reassortment in the evolution of H5N8 viruses with higher replication ability in human cells and virulence in mammals if reassortment occurred in other avian hosts (e.g. turkeys or ducks).

Data Availability

Viral genomic data is available in GISAID under accession numbers 486439, 486440 and 486441. All the other data are available upon request.

Supplementary data

Supplementary data are available at *Virus Evolution* online.

References

Abdelwhab el, S. M. et al. (2016) 'Prevalence of the C-Terminal Truncations of NS1 in Avian Influenza a Viruses and Effect on Virulence and Replication of a Highly Pathogenic H7N1 Virus in Chickens', *Virulence*, 7: 546–57.

Alexander, D. J. (2000) 'A Review of Avian Influenza in Different Bird Species', *Veterinary Microbiology*, 74: 3–13.

Arai, Y. et al. (2019) 'Genetic Compatibility of Reassortants between Avian H5N1 and H9N2 Influenza Viruses with Higher Pathogenicity in Mammals', *Journal of Virology*, 93: e01969–18.

Bolte, H. et al. (2019) 'Packaging of the Influenza Virus Genome is Governed by a Plastic Network of RNA- and Nucleoprotein-Mediated Interactions', *Journal of Virology*, 93: e01861–18.

Böttcher, E. et al. (2006) 'Proteolytic Activation of Influenza Viruses by Serine Proteases TMPRSS2 and HAT from Human Airway Epithelium', *Journal of Virology*, 80: 9896–8.

Bottcher-Friebertshauser, E. et al. (2011) 'Inhibition of Influenza Virus Infection in Human Airway Cell Cultures by an Antisense Peptide-Conjugated Morpholino Oligomer Targeting the Hemagglutinin-Activating Protease TMPRSS2', *Journal of Virology*, 85: 1554–62.

Bouvier, N. M., and Palese, P. (2008) 'The Biology of Influenza Viruses', *Vaccine*, 26: D49–53.

Bradel-Tretheway, B. G. et al. (2008) 'The Human H5N1 Influenza a Virus Polymerase Complex is Active In Vitro over a Broad Range of Temperatures, in Contrast to the WSN Complex, and This Property Can Be Attributed to the PB2 Subunit', *Journal of General Virology*, 89: 2923–32.

Breithaupt, A. et al. (2011) 'Neurotropism in Blackcaps (*Sylvia atricapilla*) and Red-Billed Queleas (*Quelea quelea*) after Highly Pathogenic Avian Influenza Virus H5N1 Infection', *Veterinary Pathology*, 48: 924–32.

Bussey, K. A. et al. (2011) 'PA Residues in the 2009 H1N1 Pandemic Influenza Virus Enhance Avian Influenza Virus Polymerase Activity in Mammalian Cells', *Journal of Virology*, 85: 7020–8.

Capel, V. et al. (2016) 'Insight into the Relationship between the Cell Culture Model, Cell Trafficking and siRNA Silencing Efficiency', *Biochemical and Biophysical Research Communications*, 477: 260–5.

Chaimayo, C. et al. (2018) 'Specificity and Functional Interplay between Influenza Virus PA-X and NS1 Shutoff Activity', *PLoS Pathogens*, 14: e1007465.

Chan, R. W. et al. (2010) 'Influenza H5N1 and H1N1 Virus Replication and Innate Immune Responses in Bronchial Epithelial Cells Are Influenced by the State of Differentiation', *PLoS One*, 5: e8713.

Chen, H. et al. (2014) 'Clinical and Epidemiological Characteristics of a Fatal Case of Avian Influenza a H10N8 Virus Infection: A Descriptive Study', *The Lancet*, 383: 714–21.

Chin, A. W. H. et al. (2014) 'Influenza a Viruses with Different Amino Acid Residues at PB2-627 Display Distinct Replication Properties In Vitro and In Vivo: Revealing the Sequence Plasticity of PB2-627 Position', *Virology*, 468–470: 545–55.

Davis, A. S. et al. (2015) 'Validation of Normal Human Bronchial Epithelial Cells as a Model for Influenza a Infections in Human Distal Trachea', *Journal of Histochemistry & Cytochemistry*, 63: 312–28.

Dittmann, J. et al. (2008) 'Influenza a Virus Strains Differ in Sensitivity to the Antiviral Action of Mx-GTPase', *Journal of Virology*, 82: 3624–31.

Freidl, G. S. et al. (2014) 'Influenza at the Animal–Human Interface: A Review of the Literature for Virological Evidence of Human Infection with Swine or Avian Influenza Viruses Other than A(H5N1)', *Euro Surveillance*, 19: 20793.

Fusaro, A. et al. (2011) 'Phylogeography and Evolutionary History of Reassortant H9N2 Viruses with Potential Human Health Implications', *Journal of Virology*, 85: 8413–21.

Gao, W. et al. (2019) 'Prevailing I292V PB2 Mutation in Avian Influenza H9N2 Virus Increases Viral Polymerase Function and Attenuates IFN-Beta Induction in Human Cells', *Journal of General Virology*, 100: 1273–81.

Gerlach, R. L. et al. (2013) 'Early Host Responses of Seasonal and Pandemic Influenza a Viruses in Primary Well-Differentiated Human Lung Epithelial Cells', *PLoS One*, 8: e78912.

Gerlach, T. et al. (2017) 'pH Optimum of Hemagglutinin-Mediated Membrane Fusion Determines Sensitivity of Influenza a Viruses to the Interferon-Induced Antiviral State and IFITMS', *Journal of Virology*, 91: e00246.

Graef, K. M. et al. (2010) 'The PB2 Subunit of the Influenza Virus RNA Polymerase Affects Virulence by Interacting with the Mitochondrial Antiviral Signaling Protein and Inhibiting Expression of Beta Interferon', *Journal of Virology*, 84: 8433–45.

Grimm, D. et al. (2007) 'Replication Fitness Determines High Virulence of Influenza a Virus in Mice Carrying Functional Mx1 Resistance Gene', *Proceedings of the National Academy of Sciences of the United States of America*, 104: 6806–11.

Guan, Y. et al. (1999) 'Molecular Characterization of H9N2 Influenza Viruses: Were They the Donors of the "Internal" Genes of H5N1 Viruses in Hong Kong?', *Proceedings of the National Academy of Sciences of the United States of America*, 96: 9363–7.

Guo, Y. J. et al. (2000) 'Characterization of the Pathogenicity of Members of the Newly Established H9N2 Influenza Virus Lineages in Asia', *Virology*, 267: 279–88.

Hagag, N. M. et al. (2019) 'Isolation of a Novel Reassortant Highly Pathogenic Avian Influenza (H5N2) Virus in Egypt', *Viruses*, 11: 565.

Hao, X. et al. (2016) 'Reassortant H5N1 Avian Influenza Viruses Containing PA or NP Gene from an H9N2 Virus Significantly Increase the Pathogenicity in Mice', *Veterinary Microbiology*, 192: 95–101.

—— et al. (2019) 'The PB2 and M Genes of Genotype S H9N2 Virus Contribute to the Enhanced Fitness of H5Nx and H7N9 Avian Influenza Viruses in Chickens', *Virology*, 535: 218–26.

Hassan, K. E. et al. (2020) 'Novel Reassortant Highly Pathogenic Avian Influenza A(H5N2) Virus in Broiler Chickens', *Emerging Infectious Diseases*, 26: 129–33.

Hayashi, T., MacDonald, L. A., and Takimoto, T. (2015a) 'Influenza a Virus Protein PA-X Contributes to Viral Growth and Suppression of the Host Antiviral and Immune Responses', *Journal of Virology*, 89: 6442–52.

—— et al. (2015b) 'Identification of Influenza a Virus PB2 Residues Involved in Enhanced Polymerase Activity and Virus Growth in Mammalian Cells at Low Temperatures', *Journal of Virology*, 89: 8042–9.

Hennion, R. M., and Hill, G. (2015) 'The Preparation of Chicken Kidney Cell Cultures for Virus Propagation', *Methods in Molecular Biology*, 1282: 57–62.

Hoffmann, B. et al. (2016) 'Riems Influenza a Typing Array (RITA): An RT-qPCR-Based Low Density Array for Subtyping Avian and Mammalian Influenza a Viruses', *Scientific Reports*, 6: 27211.

Hsu, A. C. et al. (2012) 'Critical Role of Constitutive Type I Interferon Response in Bronchial Epithelial Cell to Influenza Infection', *PLoS One*, 7: e32947.

Ishikawa, H. et al. (2010) 'IFN-Gamma Production Downstream of NKT Cell Activation in Mice Infected with Influenza Virus Enhances the Cytolytic Activities of Both NK Cells and Viral Antigen-Specific CD8+ T Cells', *Virology*, 407: 325–32.

Jiao, P. et al. (2008) 'A Single-Amino-Acid Substitution in the NS1 Protein Changes the Pathogenicity of H5N1 Avian Influenza Viruses in Mice', *Journal of Virology*, 82: 1146–54.

Kanrai, P. et al. (2016) 'Identification of Specific Residues in Avian Influenza a Virus NS1 That Enhance Viral Replication and Pathogenicity in Mammalian Systems', *Journal of General Virology*, 97: 2135–48.

Kaplan, B. S. et al. (2016) 'Novel Highly Pathogenic Avian A(H5N2) and A(H5N8) Influenza Viruses of Clade 2.3.4.4 from North America Have Limited Capacity for Replication and Transmission in Mammals', *Msphere*, 1:e00003-16.

Kim, T. S. et al. (2003) 'Induction of Interleukin-12 Production in Mouse Macrophages by Berberine, a Benzodioxoloquinolizine Alkaloid, Deviates CD4+ T Cells from a Th2 to a Th1 Response', *Immunology*, 109: 407–14.

Kim, Y. I. et al. (2014) 'Pathobiological Features of a Novel, Highly Pathogenic Avian Influenza A(H5N8) Virus', *Emerging Microbes & Infections*, 3: e75.

Kishida, N. et al. (2004) 'Co-Infection of *Staphylococcus aureus* or *Haemophilus paragallinarum* Exacerbates H9N2 Influenza a Virus Infection in Chickens', *Archives of Virology*, 149: 2095–104.

Kok, W. L. et al. (2012) 'Pivotal Advance: Invariant NKT Cells Reduce Accumulation of Inflammatory Monocytes in the Lungs and Decrease Immune-Pathology during Severe Influenza a Virus Infection', *Journal of Leukocyte Biology*, 91: 357–68.

Kreft, M. E. et al. (2015) 'The Characterization of the Human Cell Line Calu-3 under Different Culture Conditions and Its Use as an Optimized in Vitro Model to Investigate Bronchial Epithelial Function', *European Journal of Pharmaceutical Sciences*, 69: 1–9.

Kukol, A., and Hughes, D. J. (2014) 'Large-Scale Analysis of Influenza a Virus Nucleoprotein Sequence Conservation Reveals Potential Drug-Target Sites', *Virology*, 454-455: 40–7.

Kurokawa, M. et al. (1999) 'Influenza Virus Overcomes Apoptosis by Rapid Multiplication', *International Journal of Molecular Medicine*, 3: 527–30.

Kwon, H. I. et al. (2018) 'Comparison of the Pathogenic Potential of Highly Pathogenic Avian Influenza (HPAI) H5N6, and H5N8 Viruses Isolated in South Korea during the 2016-2017 Winter Season', *Emerging Microbes & Infections*, 7: 1–10.

Lee, D. H. et al. (2017) 'Evolution, Global Spread, and Pathogenicity of Highly Pathogenic Avian Influenza H5Nx Clade 2.3.4.4', *Journal of Veterinary Science*, 18: 269–80.

Lee, Y. N. et al. (2011) 'Isolation and Characterization of a Novel H9N2 Influenza Virus in Korean Native Chicken Farm', *Avian Diseases*, 55: 724–7.

—— et al. (2018) 'Evaluation of the Zoonotic Potential of Multiple Subgroups of Clade 2.3.4.4 Influenza A (H5N8) Virus', *Virology*, 516: 38–45.

Li, W., Moltedo, B., and Moran, T. M. (2012) 'Type I Interferon Induction during Influenza Virus Infection Increases Susceptibility to Secondary *Streptococcus pneumoniae* Infection by Negative Regulation of Gammadelta T Cells', *Journal of Virology*, 86: 12304–12.

Li, Z. et al. (2006) 'The NS1 Gene Contributes to the Virulence of H5N1 Avian Influenza Viruses', *Journal of Virology*, 80: 11115–23.

Liang, L. et al. (2019) 'Low Polymerase Activity Attributed to PA Drives the Acquisition of the PB2 E627K Mutation of H7N9 Avian Influenza Virus in Mammals', *mBio*, 10: e01162.

Livak, K. J., and Schmittgen, T. D. (2001) 'Analysis of Relative Gene Expression Data Using Real-Time Quantitative PCR and the 2(-Delta Delta C(T)) Method', *Methods*, 25: 402–8.

Lo, C. Y., Tang, Y. S., and Shaw, P. C. (2018) 'Structure and Function of Influenza Virus Ribonucleoprotein', *Sub-Cellular Biochemistry*, 88: 95–128.

Lowen, A. C. (2017) 'Constraints, Drivers, and Implications of Influenza a Virus Reassortment', *Annual Review of Virology*, 4: 105–21.

Lu, L., Lycett, S. J., and Leigh Brown, A. J. (2014) 'Reassortment Patterns of Avian Influenza Virus Internal Segments among Different Subtypes', *BMC Evolutionary Biology*, 14: 16.

Lujan, H. et al. (2019) 'Refining In Vitro Toxicity Models: Comparing Baseline Characteristics of Lung Cell Types', *Toxicological Sciences*, 168: 302–14.

Ma, W. et al. (2010) 'The NS Segment of an H5N1 Highly Pathogenic Avian Influenza Virus (HPAIV) Is Sufficient to Alter Replication Efficiency, Cell Tropism, and Host Range of an H7N1 HPAIV', *Journal of Virology*, 84: 2122–33.

Matrosovich, M. N. et al. (2004) 'Human and Avian Influenza Viruses Target Different Cell Types in Cultures of Human Airway Epithelium', *Proceedings of the National Academy of Sciences of the United States of America*, 101: 4620–4.

Moreira, E. A. et al. (2016) 'A Conserved Influenza a Virus Nucleoprotein Code Controls Specific Viral Genome Packaging', *Nature Communications*, 7: 12861.

Mostafa, A. et al. (2013) 'Improved Dual Promotor-Driven Reverse Genetics System for Influenza Viruses', *Journal of Virological Methods*, 193: 603–10.

—— et al. (2015) 'Efficient Generation of Recombinant Influenza a Viruses Employing a New Approach to Overcome the Genetic Instability of HA Segments', *PLoS One*, 10: e0116917.

—— et al. (2018) 'Zoonotic Potential of Influenza a Viruses: A Comprehensive Overview', *Viruses*, 10: 497.

Mulatti, P. et al. (2018) 'Integration of Genetic and Epidemiological Data to Infer H5N8 HPAI Virus Transmission Dynamics during the 2016–2017 Epidemic in Italy', *Scientific Reports*, 8: 18037.

Nagy, A., Mettenleiter, T. C., and Abdelwhab, E. M. (2017) 'A Brief Summary of the Epidemiology and Genetic Relatedness of Avian Influenza H9N2 Virus in Birds and Mammals in the Middle East and North Africa', *Epidemiology and Infection*, 145: 3320–33.

Napp, S. et al. (2018) 'Emergence and Spread of Highly Pathogenic Avian Influenza A(H5N8) in Europe in 2016–2017', *Transboundary and Emerging Diseases*, 65: 1217–26.

Ng, A. K., Wang, J. H., and Shaw, P. C. (2009) 'Structure and Sequence Analysis of Influenza a Virus Nucleoprotein', *Science in China Series C: Life Sciences*, 52: 439–49.

Nogales, A. et al. (2017) 'Interplay of PA-X and NS1 Proteins in Replication and Pathogenesis of a Temperature-Sensitive 2009 Pandemic H1N1 Influenza a Virus', *Journal of Virology*, 91: e00720.

Pan, M. et al. (2016) 'Human Infection with a Novel, Highly Pathogenic Avian Influenza A (H5N6) Virus: Virological and Clinical Findings', *Journal of Infection*, 72: 52–9.

Papazian, D., Würtzen, P. A., and Hansen, S. W. K. (2016) 'Polarized Airway Epithelial Models for Immunological Co-Culture Studies', *International Archives of Allergy and Immunology*, 170: 1–21.

Park, S. J. et al. (2015) 'Dynamic Changes in Host Gene Expression Associated with H5N8 Avian Influenza Virus Infection in Mice', *Scientific Reports*, 5: 16512.

Penski, N. et al. (2011) 'Highly Pathogenic Avian Influenza Viruses Do Not Inhibit Interferon Synthesis in Infected Chickens but Can Override the Interferon-Induced Antiviral State', *Journal of Virology*, 85: 7730–41.

Petersen, H. et al. (2018) 'NS Segment of a 1918 Influenza a Virus-Descendent Enhances Replication of H1N1pdm09 and Virus-Induced Cellular Immune Response in Mammalian and Avian Systems', *Frontiers in Microbiology*, 9: 526.

Poen, M. J. et al. (2018) 'Local Amplification of Highly Pathogenic Avian Influenza H5N8 Viruses in Wild Birds in The Netherlands, 2016–2017', *Euro Surveillance*, 23: 17–00449.

Pohlmann, A. et al. (2018) 'Swarm Incursions of Reassortants of Highly Pathogenic Avian Influenza Virus Strains H5N8 and H5N5, Clade 2.3.4.4b, Germany, Winter 2016/17', *Scientific Reports*, 8: 15.

Pu, J. et al. (2015) 'Evolution of the H9N2 Influenza Genotype That Facilitated the Genesis of the Novel H7N9 Virus', *Proceedings of the National Academy of Sciences of the United States of America*, 112: 548–53.

Pulit-Penaloza, J. A. et al. (2015) 'Pathogenesis and Transmission of Novel Highly Pathogenic Avian Influenza H5N2 and H5N8 Viruses in Ferrets and Mice', *Journal of Virology*, 89: 10286–93.

Reid, S. M. et al. (2016) 'The Detection of a Low Pathogenicity Avian Influenza Virus Subtype H9 Infection in a turkey Breeder Flock in the United Kingdom', *Avian Diseases*, 60: 126–31.

SJCEIRS-H9-Working-Group. (2013) 'Assessing the Fitness of Distinct Clades of Influenza A (H9N2) Viruses', *Emerg Microbes Infect*, 2: e75.

Stech, J. et al. (2008) 'Rapid and Reliable Universal Cloning of Influenza a Virus Genes by Target-Primed Plasmid Amplification', *Nucleic Acids Research*, 36: e139–e139.

Świętoń, E. et al. (2018) 'Genetic Characterization of H9N2 Avian Influenza Viruses Isolated from Poultry in Poland during 2013/2014', *Virus Genes*, 54: 67–76.

Szretter, K. J. et al. (2009) 'Early Control of H5N1 Influenza Virus Replication by the Type I Interferon Response in Mice', *Journal of Virology*, 83: 5825–34.

Varga, Z. T. et al. (2011) 'The Influenza Virus Protein PB1-F2 Inhibits the Induction of Type I Interferon at the Level of the MAVS Adaptor Protein', *PLoS Pathogens*, 7: e1002067.

Vigeveno, R. M. et al. (2020) 'Outbreak Severity of Highly Pathogenic Avian Influenza A(H5N8) Viruses Is Inversely Correlated to Polymerase Complex Activity and Interferon Induction', *Journal of Virology*, 94: e00375.

Wang, X. et al. (2016) 'Characteristics of Two Highly Pathogenic Avian Influenza H5N8 Viruses with Different Pathogenicity in Mice', *Archives of Virology*, 161: 3365–74.

—— et al. (2017) 'Synergistic Effect of PB2 283M and 526R Contributes to Enhanced Virulence of H5N8 Influenza Viruses in Mice', *Veterinary Research*, 48: 67.

White, M. C. et al. (2019) 'H5N8 and H7N9 Packaging Signals Constrain HA Reassortment with a Seasonal H3N2 Influenza a Virus', *Proceedings of the National Academy of Sciences of United States of America*, 116: 4611–8.

Yoneyama, M. et al. (1998) 'Direct Triggering of the Type I Interferon System by Virus Infection: Activation of a Transcription Factor Complex Containing IRF-3 and CBP/p300', *The EMBO Journal*, 17: 1087–95.

Zhao, Z. et al. (2014) 'PB2-588I Enhances 2009 H1N1 Pandemic Influenza Virus Virulence by Increasing Viral Replication and Exacerbating PB2 Inhibition of Beta Interferon Expression', *Journal of Virology*, 88: 2260–7.

Zohari, S. et al. (2010) 'Differences in the Ability to Suppress Interferon Beta Production between Allele a and Allele B NS1 Proteins from H10 Influenza a Viruses', *Virology Journal*, 7: 376.